We thank the referees for their useful comments and suggestions which have helped us to improve the manuscript. Comments from reviewer 1 are in red, reviewer 2 in blue. Our responses are in black and bullet-pointed. The main changes to the manuscript are summarised as follows:

Reviewers comments

Reviewer 1, Reviewer 2

Main Changes (see discussion below):

1. **Title updated**
2. **Figure 5 removed *(original figure numbers have been used for reference in this document)*.**
3. **Using "Case 1-7" instead of flight numbers.**
4. **Size distributions (Fig. 4) updated to show individual probe data.**
5. **Text in Sections 2.3, 3.2, 3.3 cut significantly, Section 4 text made more concise**
6. **Classification scheme included as Table S1.**

General Comments

"Exploring the variability of aerosol particle composition in the Arctic: a study from the springtime ACCACIA campaign" by Young et al. focus on the chemical composition observed during six flights conducted in spring 2013.

Reading the manuscript it is clear that the authors worked with a limited set of data. Nevertheless, any airborne observations of aerosol properties should be shared with the community, as we still lack some fundamental understanding on this topic. As pointed out, models are not yet able to fully reproduce details in the variation of the Arctic aerosol properties. Unfortunately, the authors chose to focus on low-level data, and in my opinion the most interesting conclusion was based on comparing two levels in the vertical.

- Low-altitude data was the focus of this study as particles collected were thought to be the primary contributions of INPs and CCN to the clouds in the region. It was also the aim to compare samples between flights from similar locations with respect to cloud. Below cloud filters were available for each of the 6 flights shown in this study (Fig. 1), whilst above cloud filters were only available in flights B764, B765 and B768. The only feasible below/above cloud comparison (B764) was analysed and included in this study.

The conclusion about the origin of the air in FL764 and the ubiquitous presence of minerals in all flights, are sufficient to warrant the publication of these data.

Before any publication I have a few comments that might improve the manuscript. To begin, I think the title must be revised. The "variability of aerosol particle composition"

implies some statistical representation of a larger data set than is actually presented here. In total I calculated about 1.5 hours of sampling time and less than 10 cubic meters or air. Besides some mean values, there are few statistical measures on the variability presented in the manuscript. I propose a more direct approach, where the title reads something like: Observed size dependent chemical compositions of aerosols in the sub-Arctic during six measurement flights during the ACCACIA campaign. Far from perfect suggestion, but I hope the point is made.

- Title has been updated to read as follows: “Size-segregated compositional analysis of aerosol particles collected in the European Arctic during the ACCACIA campaign.”

On the topic of variability, may I suggest the reference by Tunved et al. 2013 (ACP) for a climatology of physical properties observed at the Zeppelin station to include in your introduction. Also pertinent to this study are references from the ASTAR 2007 campaign, i.e. Hara et al.

- Citations to these articles (Hara et al. 2003 (ASTAR 2000), Tunved et al. 2013) have been included in the introduction as suggested.

This study analyzed the size distributions and element compositions of samples collected by aircraft during the springtime segment of the Aerosol Cloud Coupling and Climate Interactions in the Arctic campaign (ACCACIA). The study is important because it leads toward a better understanding of the composition of particles directly below and above clouds in the Arctic. The types of particles studied here could have served as cloud condensation nuclei or ice nucleating particles in the vicinity of Svalbard, Norway, and therefore, may lead toward a better understanding of the effect of clouds on the Arctic climate. The paper cites existing literature extensively, which normally is most helpful. However, here the literature could have been presented more concisely, and thus, for this reason alone the paper could have been shortened.

- Portions of text throughout manuscript have been shortened, see below for details.

The paper presents a substantial amount of information that was reported previously in the literature, and thus, need not be reported here. For example, Section 2.3 discusses extensively the process of analyzing particle populations with energy-dispersive x-ray spectroscopy associated with SEM. Particle population analysis by SEM has been well established for decades, including normalizing the composition by weight percent, which is the only plausible way to report composition if particle standards are impractical.

- Information pertaining to the analysis set-up in Section 2.3 has been simplified in the manuscript.

In another example where the lack of a concise explanation causes some confusion, the authors indicate in one place that carbon and oxygen were measured, but later indicate that carbon and oxygen were not quantified. More about this below under Specific Comments.

- Addressed below.

In reporting of results and the follow-up discussion, some of the interpretations are questionable or lack the appropriate emphasis. For example, I do not see where one

can draw convincing conclusions from Figure 5 about differences in the complement of particles classes between smaller particles (<0.5 um) and larger particles (>0.5 um). As the authors admit, the compositional variability is great among the samples from the different aircraft flights. The between-sample variability in Fig. 5 overwhelms any size-dependent trend. Regarding appropriate interpretive emphases, the authors make a number of definitive claims of the data showing a “clear” effect where the data are more nuanced. I recommend that the authors be more careful in interpreting their data. Specific examples are presented below.

- This is a fair point, need to be careful with language. This required some general re-wording throughout the manuscript, however a discussion usefulness of Figure 5 is mentioned below. The conclusions of the paper would be unchanged with adequate evidence if Fig. 5 was removed, therefore it has been.

Overall however, I find the paper informative because the authors do manage to return at the end of the paper to their main objective. That is, they discuss rather well (with appropriate caveats) how the size-segregated compositional analysis here relates to CCN, INPs and cloud microphysics.

1 Introduction

29407 Section 1.1 line 22
Nuclepore is a trade name. It would be good to indicate the source (i.e, manufacturer) of the filters.

- Filters used were Whatman Nuclepore track-etch membranes. The manuscript has been updated to include this information in the Methodology section (Sect. 2.2, line 134)

2 Methodology

29408 Section 2.1 paragraph 2
There is extensive particle-size overlap among the particle size distribution techniques used: PCASP, CAS-DPOL, and CDP. This suggests that for the overlap regions these probe techniques could have been compared. However, this was not done.

- Figure 4 has been updated in the manuscript to include the probe data individually, therefore allowing the regions of overlap to be viewed and compared.

2.2. Filter collection

Line 20-25
My understanding is that sub-isokinetic sampling is not the trick for removing large particles or droplets. It is the virtual impactor at the bend (where the inlet direct the sample flow through the fuselage) that gives this positive effect.

- Agreed, sub-isokinetic sampling in fact has an enhancement effect on large particles. It is the bend in the mechanism which provides inertial separation of cloud drops and rain into a bypass tube. This has been made clearer in the manuscript.

This design in itself generates a blunt cut-off in the sampling of particles, which is not addressed in this manuscript. When sampling sub-isokinetic with a forward facing probe,

this introduces a size dependent sampling efficiency which favors larger particles. How much, this effect influences depends on the ratio between the sampling flow and the volume swept through by the opening area of the inlet as the plane moves forward. How large is this ratio, and how does this potentially influence the size dependent sampling for the filter substrates?

- It is not known if the collection efficiency of the sampling mechanism has been quantified but, as stated by Formenti et al. 2008, a precise calculation would require the characterisation of the inlet in a wind tunnel. Despite this, Andreae 2000 compared ground-based and aircraft samples during the ACE-2 campaign and found the sampling efficiency of the aircraft inlet (MRF C-130 version) to be about 35% for coarse-mode aerosol. The same comparison showed good agreement for fine-mode aerosol particles. Formenti et al. 2003 use this information to set an approximate 50% cut-off diameter of 3micron for sea-salt particles collected during the SAFARI campaign (also using the MRF C-130 aircraft). Samples collected here were done so using the same mechanism investigated by these two studies, therefore this information should similarly apply in this study (with some deviation allowed for differing sampling conditions etc.). This would suggest that the coarse-mode is under-represented in these ACCACIA filter samples, whilst the collection efficiency of fine-mode aerosol is much better. This agrees with the conclusions discussed in Section 4.1, where it is speculated that it is an artefact of the SEM analysis which is causing the significant disagreement with the probe data in the accumulation mode. This conclusion was reached by Chou et al. 2008, who found good agreement between filter (analysed with TEM) and probe data on scales of a few tenths of a micron up to 0.5micron. Agreement deviated at sizes >0.5micron, where they observed significant large particle enhancement due to the sub-isokinetic sampling. Such enhancement was not observed in this study, and probe data always produced a greater concentration than the filters in the coarse mode. Given this information, the losses of coarse-mode particles appear to dominate over the enhancement effect introduced from sub-isokinetic sampling, and these efficiency issues have been emphasised further in the manuscript to make this clearer.

Even with a tapered tip (as I believe is used on the FAAM platform) there is a potential risk of drops shattering on the probe tip, or more so, inside the probe if the probe is not aligned with the streamlines of the surrounding air. That is, the probe is of axis during low speeds with high aircraft attack angles or in turns etc. These problems could cause spurious effects in the data during cloud traverses. Where any such observed, or was this problem considered in the analysis somehow?

- The filters used were exposed only during horizontal flight legs where potential angle-of-attack issues were not encountered. The aircraft speed was ~100ms^{-1} in all sampling cases, therefore this issue was not evident in the data.

2.3 Environmental scanning electron microscopy

The paper describes the use of an ESEM with EDS for analyzing the various polycarbonate filter samples. The ESEM is used in the high-vacuum mode, so it functions here as a conventional SEM with EDS. Since the instrument is not used as an ESEM, i.e., at low vacuum with a water vapor atmosphere, it should be indicated in this section that the instrument is essentially a conventional SEM to avoid confusing readers unfamiliar with an ESEM. All later mentions of ESEM in the paper should be changed to SEM.

- This is a valid point and all references to ESEM were changed to SEM in the manuscript.

29410 lines 19-21
The paper explains at length how particle are analyzed by SEM, and as mentioned above, much of this is already in the literature. There is, however, one significant gap: the software procedure used to perform the particle population analysis in the SEM should be better explained. It is stated that the electron beam is controlled by the EDS system to provide automated analysis of the sample, i.e., the analysis of the particle population on a filter. This implies that the X-ray signal is used to detect the presence of a particle and determine where in the particle spectra are to be taken. I know of no commercial software, EDAX Genesis included, that does this. Rather, software uses the backscatter electron or secondary electron signal to detect a particle. Typically, software decides where to point the beam within the particle for X-ray collection by assessing the shape of the particle and then judging where the center of the particle is. The paper fails to indicate whether the backscatter or secondary electron signal was used and whether the beam was held stationary or rastered within the particle. These issues should be made explicit in the Methodology.

- The backscatter electron signal was used. As described by the reviewer, the software identifies the particle via greyscale thresholds and locates the centre. The analysis was done in core mode, using 70% of presented area, and the beam was rastered over that area to compute each spectra. This is what we meant by an averaged spectra, however we agree that this was not clear. The text in Section 2.3 has been updated to reflect this, in lines 170-178.

29411 lines 6-7
It is indicated that carbon and oxygen are included in the analysis. However, these elements would be highly problematic because X-rays from the polycarbonate substrate would certainly penetrate the particles. The authors do mention this problem, and two paragraphs later they state that carbon and oxygen were not included. It would be clearer and more concise if the authors simply stated that carbon and oxygen were not quantified. Later the authors indicate that the presence of carbon and oxygen in an X-ray spectrum containing no other elements provided evidence that the particles were carbonaceous. Here, we are to assume that carbon and oxygen in a spectrum were used qualitatively, not quantitatively.

- We have updated Section 2.3 to reflect this request. We have stated that elements C to Zn are scanned, but C and O are presented qualitatively due to the polycarbonate filter issue. This is difficult to address as C and O measurements were made and approximate thresholds were used to identify when there were no other elements detected (See Table S1 for classification criteria), therefore the data is used. We have made this clearer to the reader in Sections 2.3 and 2.4.1.

Page 29411 Line 11
What does 4 pixels correspond to in um?

- Minimum sizes are listed in Table 3. A reference to reflect this has been included on line 180.

29411 paragraph 2 (lines 12-20)

This paragraph focuses on an analysis of a blank. More information should be provided about the nature of the blanks. For example, how many blanks were used? Were they field blanks in that they were somehow exposed in the aircraft, or were they simply lab blanks taken out of a box prior to the SEM analysis? Field blanks are much preferred in this type of study.

- One field blank filter pair from flight B762 was analysed. These were treated similarly to the exposed filters (i.e. taken aboard the aircraft) without any exposure to the air flow. The manuscript has been updated to address this (lines 191-194).

Page 29412
Last line "The number: : :" what is the fraction?

- A bug was identified in the code which had been removing more particles than first thought. Approx 3-5% more particles were removed than should have been. All of these were classified as carbonaceous once they were included in the data. This has been rectified and Fig 6 and 8 have been re-done and updated in the manuscript. The figures have changed very little but in the interest of consistency they have been re-done. The fraction of particles removed is ~4-5%, though this is variable between different filters and different scans. This information has been updated in the manuscript.

2.4 Classifications

29413 Section 2.4 and Table 4
The omission of quantitative carbon and oxygen measurement and the identification of carbonaceous particles based on the x-ray spectrum exhibiting qualitatively only carbon and oxygen has a significant drawback. Certainly, the authors were correct to avoid quantifying these elements. However, mixed-phase aged particles of carbon (organic or soot) plus mineral dust could not be classified, not to mention carbonate minerals alone. The authors should discuss this drawback and possible solutions.

- More information about the limitations of the analysis (with respect to C and O measurements) has been included in Section 2.4.1 and 4.3. Information on coatings that was originally in Section 4.3 has been moved to the introduction to emphasise its importance in the study.

The classification scheme presented in Table 4 only indicates qualitatively how particles were classified. The actual scheme had consist of numeric boundaries, i.e., weight percent boundaries. What do the following mean: "significant Na and Cl", "major fractions of Na, Cl, S", "mixtures primarily containing Si and Al", etc? It is important to report the quantitative scheme so other researchers can utilize the same scheme if desired.

- Classification scheme has been written up and included instead as a supplementary table (Table S1) due to its length.

2.4.5 Biomass tracers

Page 29417 Line 25 The word "present", is this meant to be "originated"? If not I don't get the logic of the paragraph. Surely such aerosol may be present in the Arctic.

- Such particles may be present in the Arctic, but yes it is unlikely that they originated

there. Their presence could therefore be used as an indicator for long-range transport. The text in Section 2.4.5 has been updated to make this clearer.

2.4.6 Other

Why is it implied that particles are well mixed if they are classified as other, i.e., not within the classification scheme?

- Particles unclassified by the scheme are thought to be mixes of the classifications as they had not met the specific criteria for any category. Typically, many different elements were detected in quantities not substantial enough to allow for distinct classification. As many elements were measured, these were assumed to be mixes. However, as these were typically Si and Al deficient, they were not thought to be dusts. As agreed below, these should not be referred to as “well-mixed” and this has been updated in the manuscript.

Also, the following statement is problematic: “: : : the automated scan will not catalogue the spatial dependencies and instead computes a mean spectrum for presented particle surface area.” It is important to use precise wording. Scanning in automated SEM allows for the detection of a particle from the backscattered electron or secondary electron signal. Typically, the acquired spectrum is not a mean but rather the result of the electron beam held stationary on the particle for a duration after the particle center is determined. To clarify, the authors should state that automated SEM for particle analysis does not acquire an element spatial map of each particle.

- Agreed, the wording of Section 2.4.6 has been updated to reflect the reviewers comments.

3.1 HYSPLIT back trajectories

Page 29418 Line 22 Strike “monotonically” as this is not always true and especially not for all trajectories.

- “Monotonically” has been removed from line 360.

3.2 Aerosol size and morphology

Figure 4. This figure is somewhat central to the manuscript as it is used both to corroborate different measurement technics as well as in the interpretation of the data. I understand that the probe data are means from each flights for the corresponding period of the filter samples. However, it is not clear if these are arithmetic or geometric means.

- All averages and values quoted as “averaged values” are arithmetic means of the data. These have been updated in manuscript.

Also, there are no indications of variability (some call it uncertainty) for each size bin or at least size range.

- Figure 4 has been updated in the manuscript to include the data from each individual probe with 1 standard deviation displayed. Similarly, an average of the SEM data has been overlaid on top of the scatter (x) points to make comparison easier. Only upwards error bars are included for clarity. Error bars have not been

included on the SEM data as the figure would become incoherent, however the spread is still indicated by the scatter (x) points.

The ESEM data is unclear to me. Can a similar line be produced as for the probes? What does each marker represent, fixed size range or number of particles? Presumably, these must represent some sort of histogram if they are to be dN/dlog Dp values.

- The updated version of Figure 4 displays the dN/dlogD data from the filters as an averaged line in addition to the scatter (x) points. The reviewer is correct in stating that each SEM data point represents a histogram of number concentration normalised by bin width (dN/dlogDp). The data was originally presented this way to indicate the resolution of the SEM and the large number of particles detected in each case. This is preserved in the new version of the figure.

I think I got that both filters are uses for each data point (if I'm wrong correct me). My main request is that the authors include meteorology and ambient conditions to the manuscript. It is not reported and could fit very well into a table with average T and RH for each sampling period for instance. The result of this could enter the discussion of figure 4. If the RH is high (i.e. >80%) this will significantly change the ambient vs dry aerosol apparent sizes. In some cases, the probe data could be shifted as much as a factor of 2, or more (towards smaller particles) comparing ambient and dry conditions.

- Mean temperature and RH data are now included in Tables 2 and 4. All RH values were found to be high (>90%). Temperature data does not give much to the interpretation of the data but it is helpful to contextualise the exposures. Calculated RH value for B762 (case 3) is not trusted. This may suggest condensation on the probe surface interfering with the measurements. Agreement in Figure 4 between the SEM and probe data is worst for B762 (case 3) and B764 (case 4), and these cases resulted in the greatest RH measurements. Derived RH values for B761 (case 2) and B765 (case 5) are similar even though some in-cloud sampling was definitely noted in B761 (case 2). Probe data from these cases appear to have reasonable, and arguably similar, agreement with the SEM data. Lastly, the lowest RH values were deduced in B760 (case 1) and B768 (Case 6) and, keeping with the trend, these cases provide the best agreement with the SEM data. It must be noted that the derived RH values are not dissimilar. However, these data do appear to help interpret the data, and have therefore been included in Tables 2 and 4 in the revised manuscript.

Later this figure is used in connection of "comparable" in section 5, it is important to note over what size ranges this is true and under what conditions (after the difference between ambient and dry conditions are considered).

- The text in Section 5 has been updated to refer to the comparable size ranges (~0.5micron to 10micron) and address the relevance of the derived RH values.

29420 lines 9-15
I don't think it is correct to say that the agreement between the SEM data and the probe data is clearly dependent on whether or not the cloud was sampled. There appears to be some dependence, but I would say that the out-of-cloud B765 case exhibits less agreement between the SEM and probe data than for the B761 case which had exposure to the cloud. Here, the authors should be more careful in their cause-and-effect assertion.

- This is a good point and was also raised by Reviewer 1. This has been addressed by both the updated figure, showing the variability of the probe data, and the included temperature and relative humidity data in Tables 2 and 4. The RH data helps to explain the agreement or lack thereof between the probe and SEM data, as described above. It also points out that B761 (case 2) and B765 (case 5) are not dissimilar in terms of ambient RH, so offering an explanation of the poorer agreement displayed.

What is more interesting and obvious is the lack of agreement between the SEM and probe data in most cases (the exception perhaps is B768) for particles < 1 um. Presumably, the PCASP can assess sizes down to 0.1 um while the SEM analysis can assess sizes down to 0.13 um (Table 3). We are left hanging on this issue until the Discussion section. It would have been helpful if the authors acknowledged the obvious here in Results and said something like: “more about this in the Discussion.”

- The inlet issues are suggested here as a possible explanation of the disagreement, and a link to the Discussion section has been included in line 404.

3.3 Aerosol composition

29420 Section 3.3
I am not sure what is meant by an “element index” in the first paragraph. If one simply takes the composition data normalized to weight percent in the analysis software, then the effect from the filter is not a problem.

- We are unsure of the question, so will explain the method: The analysis software produces an elemental weight percent for each element (C to Zn). C and O were included in the spectral fit to avoid spurious errors in the fitting software, therefore a measure of C and O is included in the data for each particle. As stated, this measure of C and O is not used quantitatively in main classification groups (it is used approximately in carbonaceous and biogenic, see Table S1), as the filter substrate is influencing it. To do compositional analysis on each particle, the measured weight percent of each element (Na to Zn) is normalised by either the summed total (Na to Zn) measured or a specific ratio is calculated to create a new fraction, or index, for each element. This index is what was referred to distinguish from the raw weight percentages. However, this text has been removed in the manuscript due to the inclusion of the quantified classification criteria in Table S1.

29421 and Figures 5-8
The classification data presented in Figure 5 are far less informative than data presented in Figs. 6 and 8. The only reasonable conclusion drawn from Fig. 5 is that distribution of particle classes between flights is highly variable. I do not see how the mixed chlorides and metallic classes are independent of size. I cannot agree that sulphates, carbonaceous, and biomass tracers are strongly detected in the smaller particles. There is too much between-flight variation. I would caution the authors against reading too much into Fig. 5. In fact, the authors may not want to use Fig. 5 at all.

- Fig. 5 was included to show variability between flights and indicate the number of particles detected in each size range. As pointed out, there is a lot of inter-flight variability. This variability can be seen from Fig. 6, and there are few references to Fig. 5 in the text. Therefore, Fig. 5 has been removed and the total number of

particles scanned in each case is now indicated in Fig. 6. The conclusions of the paper and evidence for them are unaffected by the removal of Fig. 5.

Figure 6 shows a clearer distinction between particles sizes based on particle classes. However, this appears to be due to the authors selecting particles sizes where there was agreement between the SEM size data and the probe data.

- In Figure 6, only sizes which showed relatively good agreement with the wing-mounted probes (0.5micron to 10micron) were included as data obtained out with this range may not be representative of the aerosol population sampled. The lack of agreement is most likely due to the efficiency issues discussed in Section 4.1. Few particles >10micron were measured in most cases; however, case B761 did have a greater number of these. In addition, it has been noted in previous studies (Kandler et al 2011) that signal-to-noise issues arise for particles <0.5micron, and the SEM interaction volume of small particles is likely to be larger than the particle itself. This data was therefore averaged (~1st size bin of Figure 6, and panel A of Fig 8) to give some indication of the composition of the small particles. This was not taken further (e.g. size segregation) as we were not confident if this data was representative given these SNR issues and the inlet/sampling issues discussed in Sections 2.2 and 4.1.

Figure 7 shows only a few “clear” distinctions: in particular, the elevated K/Al, Ca/Al, and Fe/Si levels for the B768 case. Again, I would caution the authors against making strong statements such as there being a “clear” peak in the Si/Al data for the B764 case. Yes, it is the highest mean, but the B765 mean is very close.

- Agreed, the text in Sections 3.3 and 4.2 have been updated to reflect this.

Figure 8 is perhaps the most relevant of all in this paper because of the positional importance of bands CCN and INP (below vs. above) with respect to the cloud.

4 Discussion

4.1.2 Case B768

29425 Case B768
I do not see how the authors can make the claim that Fig. 4 shows a much higher particle loading for the B768 case. The probe data B768 data are about comparable to the B765 data and perhaps less overall than the B761 data.

- This is a very good point. The size distribution of B768 (case 6) is not as dissimilar to B761 (case 2) and B765 (case 5) as the absolute number concentrations would suggest. The total number of particles for each case is quoted in new version of Fig. 6. Though the total numbers collected for this filter pair are not dissimilar to B761 (case 2), the significantly shorter sample time (4mins vs 30mins) infers the greater particle loading. The manuscript has been updated to reflect these changes.

4.3 Internally-mixed aerosol particles

This section is too verbose and contain much background information which is more pertinent into the introduction. Cut what is not essential to the findings of this study.
In my opinion there is information about minerals, but nothing about their IN potential,

which would potentially reduce this section a lot.

- Significant portion of Section 4.3 discussing mixed mineral dusts has been removed and inserted in the Introduction.

29428 Section 4.3
I do not see how one can assess with confidence the degree of internal mixing from the variability in the mean composition fractions in Fig. S1. Internal mixing suggests that particles have spatially-separated phases such as for the particle in Fig. 2. (I would disagree that this is a “well-mixed” particle!)

- Good point again, mixed yes but not well-mixed! The term “internal-mixing” has perhaps been used more loosely than it should, therefore the majority of these references have been changed to “mixed” in the manuscript.

In this paper, it seems that internal mixing is determined by the number of elements detected in the particles. As many minerals are compositionally complex, a mineral particle may be compositionally complex but with phases that are not spatially separated, and thus, the particle cannot be considered internally mixed.

- We can see the confusion, however those in the “other” category have passed through the variable criteria for minerals (Table S1), not met these, and so are unclassified. We agree minerals are compositionally complex and may contain numerous elements, yet those left in the “other” category are mostly Si and Al deficient, suggesting they are not dusts and are mixes of something else. We agree that the internally mixed hypothesis should be treated better: the text in Sections 2.4.6 and 4.3 has been updated to reflect this. The particles in the “other” category should be referred to as “mixed”, not necessarily “internally-mixed”. There is no way from this data to concretely determine whether these particles are mixed in the atmosphere or at the source; however, it could be suggested that those detected in the above-cloud case (case 7) had undergone mixing over transport due to their measurement location.

5 Conclusions

29431 lines 1-5
As stated above, conclusions drawn from Fig. 5 are not convincing. I do not see where one can say that carbonaceous particles and sulphates are prevalent in the smaller particles – more present, yes, but not prevalent.

- The text in Section 5 has been updated to refer to these categories as “mostly observed” in the sub-micron limit. As Figure 5 has been removed, the figure reference has been updated to refer to Fig. 6 instead.

Page 29431 Line 7-8
Ok until “;”, after that can be striked).

- Manuscript has been updated to reflect this change.

Page 29432 Line 2
To make my point, meteorology is used as an argument, but not reported in the manuscript. Please, include some info on T and RH at least.

- Mean temperature and RH values have been calculated and included in Tables 2 and 4 to address this.

In general it would be nice if dates for flights where used and flight numbers where referred to in the table and not vice versa. It makes much more sense to other people not specifically involved in the campaign.

- Table 1 updated to reference each below-cloud case as 1-6 rather than use flight numbers. The above cloud case discussed in Sect. 3.4 has been updated to case 7. This should make the number of samples analysed more obvious to the reader. References to each filter pair sampled throughout the text have been updated to reflect these changes.

Given the relatively short sampling times, the trajectory analysis could be greatly simplified by fewer trajectories over the actual sampling time. The 30s interval brings no additional information and only clutters the graphs. Trajectory at start and at end would probably be more than sufficient for the analysis and conclusions.

- The small temporal interval does clutter the graphs somewhat, making B764 (case 4) and B765 (case 5) especially quite difficult to see. A new version of the figure with the reviewers suggestion, i.e. trajectory at start and end of exposure, has been made and included in the manuscript. Some of the variability in B762 (case 3) and B768 (case 6) is lost, but this isn't important to the conclusions of the paper.

It took me some time to understand the samples available. First I thought it was six, then an extra showed up. It is also not clear how many particles were analyzed per filter. Can these things be made clearer in the text/tables perhaps?

- The text in Sect. 1.1 and Table 1 has been updated to make the number of cases considered more obvious to the reader (lines 97-100). Particle numbers are indicated in Table 3 (total) and Fig. 6 (per case). References have been included in Section 2.3 (line 189) and text updated to make this more obvious.

Manuscript prepared for Atmos. Chem. Phys.
with version 2014/09/16 7.15 Copernicus papers of the LaTeX class copernicus.cls.
Date: 10 February 2016

Size-segregated compositional analysis of aerosol particles collected in the European Arctic during the ACCACIA campaign

G. Young[1,*], H. M. Jones[1], E. Darbyshire[1], K. J. Baustian[2], J. B. McQuaid[2], K. N. Bower[1], P. J. Connolly[1], M. W. Gallagher[1], and T. W. Choularton[1]

[1]Centre for Atmospheric Science, University of Manchester, Manchester, UK
[2]School of Earth and Environment, University of Leeds, Leeds, UK
[*]*Invited contribution by G. Young, recipient of the EGU Young Scientists Outstanding Poster Paper Award 2015.*

Correspondence to: Gillian Young (gillian.young@manchester.ac.uk)

Abstract.

Single-particle compositional analysis of filter samples collected on-board the FAAM BAe-146 aircraft is presented for six flights during the springtime Aerosol-Cloud Coupling and Climate Interactions in the Arctic (ACCACIA) campaign (March–April 2013). Scanning electron microscopy was utilised to derive size distributions and size-segregated particle compositions. These data were compared to corresponding data from wing-mounted optical particle counters and reasonable agreement between the calculated number size distributions was found. Significant variability in composition was observed, with differing external and internal mixing identified, between air mass trajectory cases based on HYSPLIT analyses. Dominant particle classes were silicate-based dusts and sea salts, with particles notably rich in K and Ca detected in one case. Source regions varied from the Arctic Ocean and Greenland through to northern Russia and the European continent. Good agreement between the back trajectories was mirrored by comparable compositional trends between samples. Silicate dusts were identified in all cases, and the elemental composition of the dust was consistent for all samples except one. It is hypothesised that long-range, high-altitude transport was primarily responsible for this dust, with likely sources including the Asian arid regions.

1 Introduction

The response of the Arctic environment to the changing climate has received increased interest in recent years due to the visible loss in sea-ice volume over the past three decades (e.g. Serreze et al., 2007; Perovich et al., 2008). The polar regions of our planet have a unique response to a warming

atmosphere due to environmental characteristics vastly different to the mid-latitudes, including high surface albedo and strong variability in annual solar radiation. These factors cause the Arctic to respond to climatic changes at a heightened pace (Curry et al., 1996). The complexity of the Arctic environment requires detailed observations to further our understanding of the feedbacks and underlying processes involved; however, the ability to carry out such studies is hampered by the remote location which is difficult for in-situ investigation.

Existing numerical models do not effectively reproduce the changing Arctic environment. Discrepancies in forecasted sea-ice coverage, and predicted dates for 100 % loss, are due to a variety of uncertainties within the models themselves (e.g. de Boer et al., 2014). A key uncertainty in our ability to climatologically model how these changes will progress is in our representation of atmospheric aerosol-cloud interactions (IPCC AR5, 2013). Aerosols play an important role in the Arctic radiative balance, and their influence is thought to be amplified by the unique environmental conditions of this region (Quinn et al., 2007). The annual cycle of aerosol concentration in the Arctic varies significantly by season – with highs in spring of approximately 4–5 times that observed in late summer (Heintzenberg et al., 1986) – and such variability impacts the microphysics of the mixed-phase clouds commonly observed (Verlinde et al., 2007).

The interaction of aerosol particles with clouds as Ice Nucleating Particles (INPs) or Cloud Condensation Nuclei (CCN) is dependent upon properties such as their size, hygroscopicity and composition (Pruppacher and Klett, 1997). The ability of aerosol to contribute towards microphysical structure via these pathways can have a net influence on factors such as the cloud optical depth, ice crystal/droplet number or droplet effective radius (Zhao et al., 2012); properties which can significantly affect the net radiative impact of the cloud (Curry et al., 1996). The study of INPs has developed significantly in recent years via laboratory and field studies (DeMott et al., 2010; Hoose and Möhler, 2012). It is still not clear which properties of aerosol particles promote them to act as INPs in the atmosphere. They are generally thought to be insoluble; super-micron in size; have a similar molecular structure to ice (Pruppacher and Klett, 1997); and have the potential to produce chemical bonds with ice molecules at their surface (Murray et al., 2012). For example, mineral dusts are known INPs and are used regularly in laboratory studies of ice nucleation (e.g. Zimmermann et al., 2008; Connolly et al., 2009; Kanji et al., 2013; Yakobi-Hancock et al., 2013). Sources of these particles are not ubiquitous across the globe. Internally-mixed particles can also act as INPs or (Giant) CCN. A complex particle is difficult to clearly categorise as an INP or CCN as its nucleation will be heavily dependent on the environmental conditions. The presence of coatings on particles can also have a significant impact on their role in aerosol-cloud interactions. Coatings of soluble material could enhance CCN ability and promote secondary ice production via the formation of large cloud drops (Levin et al. 1996), whilst organic coatings could suppress the nucleating ability of an efficient INP (Möhler et al., 2008). It is not well understood which particles, in which mixing state – and from which sources – facilitate ice nucleation in the Arctic atmosphere.

Previous studies of Arctic aerosol have indicated that the population is primarily composed of organic material, continental pollutants (e.g. as sulphate or nitrate gases), crustal minerals and locally-sourced species such as sea salt (Barrie, 1986; Hara et al., 2003; Behrenfeldt et al., 2008; Geng et al., 2010; Weinbruch et al., 2012). There are a wide range of sources which may contribute to this population and it is difficult to quantify the impact of different regions. ~~Some year-round~~ Extended studies of Arctic aerosol have been conducted which consider the differences in particle properties between seasons, showing that the annual cycle of aerosol particle composition (Ström et al., 2003; Weinbruch et al., 2012) and concentration (Ström et al., 2003; Tunved et al., 2013) is dominated by the influence of the Arctic Haze (Barrie, 1986; Shaw, 1995). Between February and April, an influx of aerosol from anthropogenic sources becomes trapped in the stable Arctic atmosphere and persists for long periods of time (up to several weeks) before being removed by precipitation processes (Shaw, 1995). Spring in the European Arctic is routinely characterised by these high particle number concentrations, dominated by the accumulation mode, and low precipitation rates with comparison to summer, autumn and winter (Tunved et al. 2013). During this time, ~~the particle concentrations reach a plateau and~~ the aerosol~~s~~ particles present have the potential to interact with other species, grow and develop with a low chance of being removed from the atmosphere. This promotes an enhanced state of mixing (e.g. Hara et al., 2003), which compounds the difficulty in understanding how these particles interact with the clouds in the region. It is thought that the European continent is the primary source of this aerosol, with only small contributions from North America and Asia (Rahn, 1981); however, long-range transport from the Asian continent has been found to sporadically contribute to this phenomenon (Liu et al., 2015). ~~In addition to the pollutants (e.g. as sulphate or nitrate gases), some crustal minerals have been identified in these haze events (Barrie, 1986)~~. Improving our understanding of the properties of these particles will help us to comprehend how they influence the clouds of the Arctic, and a strong method of achieving this is by identifying their chemical composition ~~of the aerosol particles present in the region~~ (Andreae and Rosenfeld, 2008).

The influence of aerosol-cloud interactions on cloud microphysical structure and the Arctic radiative budget is uncertain (Vihma et al., 2014). By improving our knowledge of these processes via in-situ observational studies in the Arctic, it is possible to reduce this uncertainty and develop models to produce a more accurate representation of the region's response to anthropogenic climate change. To this end, the Aerosol-Cloud Coupling and Climate Interactions in the Arctic (ACCACIA) campaign was carried out in the European Arctic in 2013, utilising airborne- and ship-based measurements to collect a detailed dataset of the Arctic atmosphere. The campaign was split into spring and summer segments, completed in Mar-Apr and July of 2013 respectively. During the spring section of the campaign, the FAAM BAe-146 atmospheric research aircraft was flown in the vicinity of Svalbard, Norway, with the capability of collecting in-situ samples of aerosol particles on filters. This study presents the analysis of the filter samples collected during this campaign, with a focus

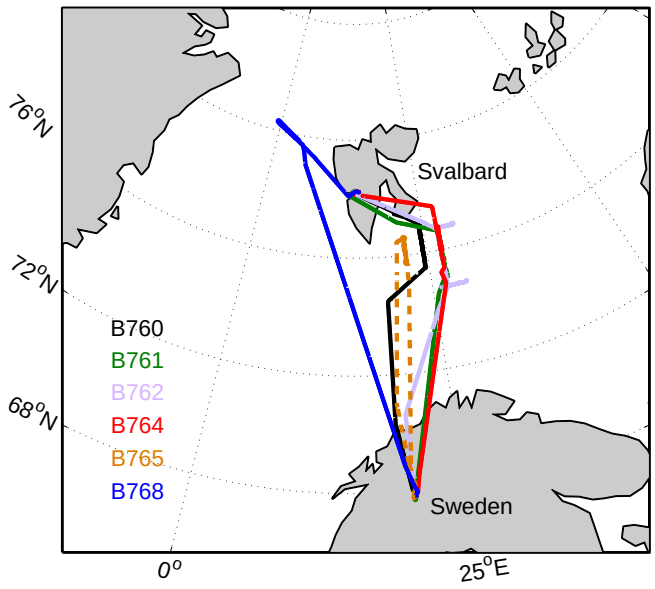

Figure 1: ACCACIA flight tracks of the main science periods undertaken for each flight where aerosol composition analysis was conducted.

placed upon identifying the compositional properties and sources of the non-volatile, coarse-mode aerosol particles present in the atmosphere during the Arctic spring.

1.1 Campaign Overview

The flights of the springtime ACCACIA campaign were mainly conducted ~~in the region~~ to the south-east of Svalbard, with the exception of flight B768 which was carried out to the north-west near the boundary with Greenland. Figure 1 details the science sections of each of the springtime flights of interest, with direction from Svalbard to Kiruna, Sweden in all cases except B765, and the corresponding dates are listed in Table 1. For the majority of these flights, a focus was placed on obtaining atmospheric measurements over the marginal ice zone between the sea-ice and the ocean, allowing the variation of cloud structure with surface conditions to be investigated.

As part of the springtime campaign, 47mm-diameter Nuclepore polycarbonate filters were exposed on-board the FAAM BAe-146 aircraft to collect in-situ samples of ~~the~~ accumulation- and coarse-mode aerosol particles (sizes $\sim 0.1\,\mu m$ to $\sim 10\,\mu m$). Such particle sizes are approximately applicable to the study of CCN and INPs (Pruppacher and Klett, 1997). This study presents the analysis of ~~one set of filters from each of the flights shown in Fig.1,~~ these aircraft filters placed in the context of how the characterised particles may interact with the cloud microphysics in the re-

Table 1: Details of FAAM flights undertaken during the spring segment of the ACCACIA campaign which had viable filter exposures. Corresponding filter case studies per flight are listed for reference.

Flight number	Date (2013)	Flight region[a] ~~with respect to Svalbard~~	Case studies
B760	21 Mar	South-East	1
B761	22 Mar	South-East	2
B762	23 Mar	South-East	3
B764	29 Mar	South-East	4,7
B765	30 Mar	South	5
B768	3 Apr	North-West	6

[a] With respect to Svalbard.

gion. Analysis of one below-cloud set of filters from each case is shown, followed by a comparison between a below- and above-cloud pair from a single case study.

2 Methodology

2.1 Aircraft Instrumentation and Trajectory Analysis

During the spring section of the ACCACIA campaign, a range of cloud microphysics and aerosol instrumentation were used on board the FAAM BAe-146 aircraft to produce a detailed record of the observed Arctic atmosphere (as described by Liu et al., 2015; Lloyd et al., 2015). In this study, data from the Cloud Droplet Probe (CDP-100 Version 2, Droplet Measurement Technologies (DMT), Lance et al., 2010), the Cloud Aerosol Spectrometer with Depolarisation (CAS-DPOL, DMT, Glen and Brooks, 2013) and the Passive Cavity Aerosol Spectrometer Probe (PCASP 100-X, DMT, Rosenberg et al., 2012) are used to provide context for and a comparison to the filter measurements.

The accumulation-mode aerosol distribution was monitored by the PCASP, whereas the CAS-DPOL measured both coarse-mode aerosol and, along with the CDP, cloud droplet number concentration. These externally-mounted aircraft probes size and count their relative species via forward-scattering of the incident laser light through angles 35–120° and ∼4–12° (for both the CDP and CAS-DPOL) respectively. The PCASP measures particle concentrations and sizes in the range of 0.1 to 3 µm, the CAS-DPOL provides similar measurements from 0.6 to 50 µm (Glen and Brooks, 2013), and the CDP measures cloud droplets from 3 to 50 µm (Rosenberg et al., 2012).

Out of cloud, the CDP and may be used to provide an indication of the wet-mode diameter of coarse-mode ambient aerosol particles. The CAS-DPOL also measures coarse-mode aerosol concentrations when out of cloud. Within cloud, the liquid-water content (LWC) can be derived from the observations of cloud droplet size. In this study, a LWC threshold of $\leq 0.01\ \mathrm{g\,m^{-3}}$, derived from

CDP measurements was employed to distinguish between out-of-cloud and in-cloud measurements, and this threshold was applied to the CAS-DPOL, CDP and PCASP data to obtain an estimate of the ambient aerosol size distributions. These out-of-cloud observations are used in this study to validate the collection efficiency of the filter inlet system.

In addition to the in-situ data gained from the instrumentation aboard the aircraft, back trajectory analyses were carried out to further contextualise the filter exposures. This was achieved using HYSPLIT 4 (Draxler and Hess, 1998), in a similar manner to Liu et al. (2015). Horizontal and vertical wind fields were derived from GDAS reanalysis meteorology (NOAA Air Resources Laboratory, Boulder, CO, USA) and used to calculate trajectories at 30 s intervals along the FAAM BAe-146 flight path. This analysis allows the direction of the air mass to be inferred; however, it does not explicitly account for turbulent motions along the derived path and therefore carries a degree of uncertainty (Fleming et al., 2012). Trajectories dating back 6 days are presented to provide an indication of the source regions of the particles collected during the ACCACIA filter exposures.

2.2 Filter Collection

The filter collection mechanism on the FAAM BAe-146 aircraft comprises a stacked-filter unit (SFU) which allows for two filters (Whatman Nuclepore track etch membranes) to be exposed simultaneously to the air stream, allowing aerosol particles to be collected on both. In the ACCACIA campaign, a combination of two filters with different nominal pore sizes was used in each exposure – a 10 µm-pore filter was stacked in front of a 1 µm-pore filter – allowing sub-micron aerosol particles that may pass through the pores of the first to be collected by the second. This mechanism allows for the approximate splitting of the total aerosol size distribution onto two filters.

The design of the inlet follows the same specifications as the MRF C-130 aircraft filtration system described extensively by Andreae et al. (2000) and ~~allows for~~ sub-isokinetic sampling~~, thus removing l~~ conditions were maintained, leading to a potential coarse-mode enhancement artefact (Chou et al. 2008). Large cloud droplets are removed from the sampled air using a bypass tube ~~and~~ , therefore ~~minimising any particulate~~ contamination from ~~cloud~~ droplets or rain is minimised (Chou et al., 2008; Johnson et al., 2012). Due to this design, large particles (> 10 µm) are also thought to be removed from the collected sample, though the collection efficiency of the entire system is not known to have been formally quantified (Formenti et al., 2008; Johnson et al., 2012). Andreae et al. (2000) estimated the sampling efficiency of the inlet to be 35% by mass for the coarse mode, with a 50% cut-off threshold of $\sim 3\mu$m (Formenti et al., 2003) and no losses identified for the accumulation mode. Chou et al. (2008) demonstrated that data collected via this inlet deviated from externally-mounted particle counters above ~ 0.5 μm, after which the coarse-mode enhancement on the filter samples becomes evident.~~Despite this,~~ Additionally, the efficiencies of the filters themselves can be estimated: the 50 % cut-off diameter of the 10 µm Nuclepore filter is approximately 0.8–1 µm at the mean face velocity encountered during this study (~ 100 cm s^{-1}) (John et al., 1983; Crosier

Table 2: Summary of sampling conditions during each filter exposure. The geographic positions are also listed. Values quoted are ~~averaged quantities~~ arithmetic means, with 1σ in brackets where appropriate. In-situ temperature and derived RH data were collected using a Rosemount de-iced temperature sensor and Buck CR2 hygrometer.

Case	Conditions sampled	Exposure Length (s)	Volume of Air (sL)	Latitude (°N)	Longitude (°E)	Altitude (m)	Temperature (°C)	RH (%)
1	Clear	600	2312.3[b]	76.2	24.5	102 (5)	-11	91.9
2	Clear[a]	1700	2608.4	76.4	26.5	238 (107)	-8	96.8
3	Cloud haze	660	826.4	76.8	28.0	375 (5)	-18	108.4[c]
4	Clear[a]	540	754.8	76.6	27.2	91 (86)	-9	97.4
5	Clear	961	1249.3	76.2	22.0	71 (18)	-9	96.5
6	Clear	240	272.7	79.9	2.8	98 (44)	-8	95.3

[a] Filter was collected mostly under clear conditions, although some in-cloud sampling was encountered at the end of the exposure.
[b] The total volume of air sampled ~~by B760~~ during case 1 is high given its exposure length due to higher-than-average flow rates applied during that flight.
[c] Contaminated measurement, likely due to condensation on detection surface.

et al., 2007), whilst the 1 µm filter has a 50 % collection efficiency at approximately 0.2 µm (Liu and Lee, 1976). ~~Qualitatively, this sampling method has been found to compare reasonably well with wing-mounted particle counters (Chou et al. 2008; Johnson et al. 2012.~~

The filters were ~~typically~~ exposed on straight, level runs for approximately 10–30 min to obtain a sufficient sample for chemically-speciated mass loadings. Although the filter system was designed to remove cloud droplets, the filters were primarily exposed out of cloud to further minimise the potential for contamination. Chosen filters were all exposed within the boundary layer (< 1000 m, see Tables 2 and 4) with no dependence on whether the surface was sea-ice covered or open ocean. Samples from below cloud were preferentially studied in this investigation (cases 1–6) as they likely included the main contributions of CCN and INPs at this time of year; however, one exposure from above cloud (case 7) is considered in Sect. 3.4.

2.3 ~~Environmental~~ Scanning Electron Microscopy

Using a Phillips FEI XL30 Environmental Scanning Electron Microscope with Field-Emission Gun (ESEM-FEG) in partnership with an Energy-Dispersive X-Ray Spectroscopy (EDS) system, automated single-particle analysis of the ACCACIA filter samples was undertaken at the University of Manchester's Williamson Research Centre (Hand et al., 2010; Johnson et al., 2012).

~~The coupled EDS system allows for morphological and compositional single-particle analysis. The electron beam is controlled by the EDS system to provide automated analysis of the sample and record detailed data of each particle imaged. The resultant compositional output is a relative~~

~~elemental weight percentage of each measured element – summed to a total of 100 % – derived from the X-ray spectrum recorded by~~ The coupled EDS system moves the sample stage through a pre-set grid to produce automated particle analysis of each sample. The software detects particles via the intensity of the back-scattered electron signal. ~~of the resultant image and allows the particles to be viewed under grey-scale contrast with the approximately uniform composition of the background filter~~ Grey-scale thresholds were set to identify particles under contrast with the background filter. The electron beam was then rastered over 70 % of the detected particle surface to produce an X-ray spectrum: relative elemental weight percentages of elements from C to Zn were recorded from the spectrum, measured and fitted with the EDAX™ Genesis software. ~~To compute each elemental weight percentage~~ For each measurement, a standardless ZAF correction method was applied; corrections which relate to atomic number, absorption and fluorescence respectively. ~~The p~~ Parameters chosen for this analysis are listed in Table 3. ~~and a~~ A carbon-coating was applied to each sample to allow ~~the analysis to be carried out using the~~ high vacuum mode to be used. ~~Contributions from the following elements were for each particle detected: C, O, Na, Mg, Al, Si, P, S, Cl, K, Ca, Ti, Cr, Fe, Ni, Cu and Zn. The primary morphological properties computed by the EDS analysis include average diameter, shape and aspect ratio. These are derived from the particle area measured by the software, which itself is determined from the number of pixels illuminated per particle analysed.~~ The minimum particle sizes detectable by each scan correspond to 4 pixels in the given image and are listed in Table 3. The total number of particles scanned by the seven cases presented in this study is also listed in Table 3.

~~Additionally, t~~ To act as a calibration, a blank filter pair was also analysed as Nuclepore filters have been shown to carry contaminants ~~themselves~~ (Behrenfeldt et al., 2008). These were taken aboard the aircraft and treated similarly to the exposed filters. A small number of particles were identified~~, yet they~~ : these appeared almost transparent under contrast and the majority produced a spectra similar to the background filter when analysed. Amongst the remaining particles, there was a notable metallic influence and some particles were found to have moderate Cr or Fe fractions. This mirrors the result presented by Behrenfeldt et al. (2008) and their presence casts doubt over the origin of particles displaying this signature in the real data cases; however, these particles were found to be few in number and so should not greatly affect the outcome of this analysis.

~~This technique has been applied by several studies (e.g. Kandler et al. 2007; Hand et al. 2010; Formenti et al. 2011; Weinbruch et al. 2012) to investigate the chemical composition of particles from a variety of sources. These~~ Previous studies (e.g. Kandler et al., 2007; Hand et al., 2010; Formenti et al., 2011; Weinbruch et al., 2012) have shown that there are ~~some~~ limitations to consider with this technique. ~~In general, the ESEM/EDS system is capable of quantifying the weight percentage of any element of an atomic number $Z > 4$ (Beryllium) (Formenti et al. 2011). The filters used in the ACCACIA campaign are primarily composed of C and O, thus they contaminate the measurements of these elements in each particle. Previous studies which have used these polycarbonate filters have~~

Table 3: Main parameters applied with ~~E~~SEM and EDAX™ Genesis software to carry out analysis of the ACCACIA aircraft filters.

~~E~~SEM/EDAX™ Genesis Analysis Parameters		
Beam voltage (kV)	15	
Working distance (mm)	10	
Operating current (µA)	~ 200	
Beam spot size	4	
Image resolution (px)	1024×800	
~~Particle coverage~~	~~70 %~~	
Total number of particles	139 630	
Magnifications applied	4000×	1000×
Filters analysed	1 and 10 µm	10 µm
Min. particle size (µm)	0.13	0.52
Field sizes (mm)	0.059×0.046	0.237×0.185

~~excluded precise measurements of carbon and oxygen from their analysis to combat this issue (e.g. Krejci et al. 2005; Behrenfeldt et al. 2008; Hand et al. 2010).~~ The polycarbonate filters used during ACCACIA produce contaminated measurements of C and O in each particle detected. Studies using these filters have excluded C and O from their analysis to combat this issue (e.g. Krejci et al. 2005; Behrenfeldt et al. 2008; Hand et al. 2010). In this study, approximate thresholds of C and O are used to identify carbonaceous species. However, only elements with $Z > 11$ (Sodium) are used precisely within the classification scheme for the compositional analysis presented.

The electron beam produced by the ~~E~~SEM can negatively interact with some particle species, causing them to deform (Behrenfeldt et al., 2008). This ~~visible deformation~~ is caused by the evaporation of the volatile components of the particles, either under the electron beam or as a result of the high vacuum (Li et al., 2003; Krejci et al., 2005). Little can be done to prevent this and it is especially difficult to manage when applying ~~the~~ automated particle analysis ~~method used in this study~~. Behrenfeldt et al. (2008) ~~investigated~~ found that this phenomenon ~~and found that it~~ only had a small impact on their results and could be disregarded. As a result, it can ~~therefore~~ be assumed that the particles analysed by this method are dry and that any volatile components will have evaporated (Li et al., 2003). There are also several implicit factors which may contribute some degree of uncertainty to the quantitative composition measurements gained. For example, errors can be introduced by uncertainties in the spectral fitting of the EDAX™ software (Krejci et al., 2005) or from the differing geometries of the individual particles measured (Kandler et al., 2007). Also, compositional data for particles less than 0.5 µm ~~should be treated with caution due to~~ suffers from increased uncertainty ~~at smaller sizes~~ (Kandler et al., 2011). ~~As with the study by Kandler et al. (2007), t~~ The sample

sizes considered here were too large to consider individual corrections, therefore the ~~compositions achieved by~~ measurements from the EDS analysis were taken as approximate values. Similarly, manual inspection of the images and spectra ~~, as carried out by Hand et al. 2010,~~ was not feasible due to the sample size and so an algorithm was imposed to remove any filter artefacts. These were typically a result of the software misclassifying the filter background as a particle itself and therefore displayed only the distinctive background signature. This background spectrum presented different characteristics than those considered to be carbon-based; the artefacts were noisy, with very low detections in all but a few of the elements, whereas the particles thought to be carbonaceous displayed zero counts in some elements as expected. The ~~number~~ fraction of detected particles removed by this algorithm was typically low (∼4–5%) ~~and~~ yet it is not possible to conclude if any real particles were removed. Krejci et al. (2005) placed an estimate of the total error involved with this technique to be around 10 % and found this value to be dependent on the sample and elements analysed. These approximations are acknowledged in the different analysis methods applied to the data in this study.

2.4 Classifications

Elemental information gained from EDS analysis can be taken further to identify particle species relevant to the atmosphere. These may typically include organic material, black carbon, mineral dusts and/or sea salt, dependent on the measurement location.

The classification scheme applied in this investigation was derived from a variety of sources (e.g. Krejci et al., 2005; Geng et al., 2010; Hand et al., 2010); however, it is most prominently based upon the detailed scheme presented by Kandler et al. (2011). ~~The main criteria of t~~This scheme ~~are summarised~~ is detailed in Table S1.

2.4.1 Carbonaceous and Biogenic

Approximate thresholds of C and O were included in this study to distinguish carbonaceous particles:. ~~A crucial property of the classification scheme adopted by~~ Mamane and Noll (1985) ~~is that they~~ considered particles with only C and O measurements to be organic or biological in nature. This approach has been adopted by other studies which applied a polycarbonate substrate (e.g. Kandler et al., 2007; Behrenfeldt et al., 2008; Hand et al., 2010). For example, particles included in this category could be soot particles or pollen grains (Behrenfeldt et al., 2008). Soot has been previously identified by introducing other properties into the classification process; for example, Hara et al. (2003) and Hand et al. (2010) categorise it via its characteristic chain-aggregate morphology. Due to the sample size, inspection of particle morphologies was not feasible in this study, therefore soot was not categorised.

Mamane and Noll (1985) developed this idea to segregate between carbonaceous and biogenic as they found a high quantity of measurable coarse-mode pollen grains in their samples. These were found to be dominated by carbon and have high spectral backgrounds with distinctive small peaks in

P, S, K and/or Ca. The study by Geng et al. (2010) utilises a comparable threshold to make a similar distinction; however, they also consider small amounts of Cl, S, K, N and/or P as indicators as these elements are important nutrients for plant life (Steinnes et al., 2000).

The carbonaceous and biogenic classifications likely include particles that may have some volatile component which cannot be measured by this technique (see Sect. 2.3), therefore the partial or complete evaporation of these particles will consequently cause the presented fraction to be a lower-limit, i.e. only the non-volatile cases can be measured. Coupled with the difficulty of distinguishing these particles from the filter background, it is important to note that the ~~particle~~ fractions of ~~the~~ carbonaceous and biogenic classes presented by this study are approximations which are likely underestimating the true organic loading on these filters.

2.4.2 Sulphates, Fresh and Mixed Chlorides

Sodium Chloride from sea salt (NaCl) can enter the atmosphere as a consequence of sea-surface winds and these particles remain predominantly sodium- and chlorine-based for a short period of time. The lifetime of Cl is hindered by the tendency of these particles to accumulate sulphate in the atmosphere, thus producing particles primarily composed of Na-S as identified by Hand et al. (2010). Due to the short lifetime of this Cl source in the atmosphere, its presence is often used to indicate a fresh contribution from the sea surface (Hand et al., 2010). It is a common conclusion that a lack of Cl-containing particles and/or a significant fraction of S in a particulate sample is suggestive of aged aerosol (Behrenfeldt et al., 2008; Hand et al., 2010).

These aged species can infer an anthropogenic influence in a sample, as they are thought to require a reaction with sulphur or nitrogen oxides (Geng et al., 2010). However, the Arctic ocean is a source of dimethylsulphide (DMS); a gas which can also interact in the atmosphere to form sulphur dioxide. The contribution of this source is greater during the summer months due to decreased sea-ice (Quinn et al., 2007), and therefore is thought to have little influence during the dates of this study. The gas source cannot be concluded here but it can be stated that Na-S particles will have been present in the atmosphere for a sufficient length of time to allow the interaction to take place. In this study, the mixed chlorides category requires that the particles must still be predominantly Na- and Cl- based, with a notable S contribution. This category also accounts for metallic contributions to the base NaCl species. The sulphates and fresh chloride categories are limited to the extremes of this distribution, with only S- and Cl-dominated signatures allowed respectively.

2.4.3 Silicates, Mixed Silicates, Ca-rich and Gypsum

Complex internal mixing in particles is often indicative of a natural origin (e.g. Conny and Norris, 2011; Hoose and Möhler, 2012); however, coagulated particles can also be produced by high-temperature anthropogenic activities. Studies have indicated that a strong method of sourcing internally-mixed particles could involve the identification of silicon: particles consisting of this element and

various mixed metals are likely to be naturally-occurring mineral dusts, and industrial by-products may lack this element in high quantities (Conny and Norris, 2011). Mineral dusts are typically composed of a variety of elements and tend to include significant fractions of Si and Al, with more minor contributions from Na, Mg, K, Ca and/or Fe amongst others.

Dusts are crucial constituents of the aerosol population as they are proven Ice Nucleating Particles (INPs) (Zimmermann et al., 2008; Murray et al., 2012; Yakobi-Hancock et al., 2013). However, they can also act as Cloud Condensation Nuclei (CCN); Ca-based dusts have been shown to react with nitrates in the atmosphere to produce hygroscopic particles that may act as CCN (Krueger et al., 2003). The concentrations of nitrates in the Arctic during March (measured at the Alert sampling station in Canada) followed an increasing trend over 1990–2003 (Quinn et al., 2007), suggesting there is some probability that this interaction could take place in this environment. Alternatively, under specific environmental conditions, internally-mixed particles consisting of dusts, sulphates and sea salt can act as Giant CCN (Andreae and Rosenfeld, 2008). In this study, the presence of such particles may be inferred by the additional detection of S or Cl with the typical dust-like signatures. This can occur if the dust in question has been transported over long distances and thus undergone cloud processing or acidification reactions (Mamane and Noll, 1985; Behrenfeldt et al., 2008). Or, more simply, these could be the result of a sea salt or sulphate coating on a mineral dust particle, and such mixtures have been modelled to have significant effects on warm clouds by augmenting the CCN population (Levin et al., 2005). Complex internal mixtures containing Si, S and/or Cl are therefore indicated in this study under the classification mixed silicates.

It is difficult to identify particular species of mineral dusts using the EDS method as these particles are closely related compositionally; there are minimal differences between the chemical formulae of some dusts and this may not be accurately detectable by the method. In several studies (e.g. Kandler et al., 2007; Hand et al., 2010), the specific phases of the mineral dusts observed were not quantified, instead they considered both the individual X-ray counts and ratios between the elements measured to classify their sampled particles into set groups such as silicates and carbonates. It has often been considered that Al, Ca and K are indicative of aluminosilicates (such as Kaolinite), carbonate minerals – such as Calcite ($CaCO_3$) and Dolomite ($CaMg(CO_3)_2$) – and clays/feldspars respectively (Formenti et al., 2011). Due to the lack of a sound quantitative measure of C, carbonate minerals were inferred from their Ca and Mg abundances in this study. Some mineral classes have a distinct elemental relationship and these may be easier to classify; for example, Gypsum ($CaSO_4 \cdot 2H_2O$) samples typically do not deviate from their base chemical formulae whereas others (especially amongst the aluminosilicates) can vary widely (Kandler et al., 2007). By this reasoning, Gypsum was included as its own classification, whereas the vast majority of mineral dusts observed were grouped into the silicates, mixed silicates and Ca-rich categories, dependent on the relative quantities of Si, S and Ca they contained.

2.4.4 Phosphates and Metallics

These groups include particles with significant influences from phosphorus and transition metals respectively. Particles classified as phosphates in this study may include those composed of Apatite – a Ca- and P-based mineral group – as factories tailored towards processing these minerals are common in the nearby Kola Peninsula, Russia (Reimann et al., 2000).

The presence of transition metals in the collected particles can be viewed as an indicator for an industrial origin (Weinbruch et al., 2012). In this study, potential anthropogenic local sources for the metallic particles may be the coal burning facilities on Svalbard (in Longyearbyen and Barentsburg) or various metal smelters in the Kola Peninsula, Russia (Weinbruch et al., 2012). The metals included in the EDS analysis were Ti, Cr, Fe, Ni, Cu and Zn. Contributions from these may be attributable to anthropogenic and/or natural sources and could be in the form of metal oxides or constituents of complex minerals (Hand et al., 2010). For example, Fe can occur naturally and is common within clay minerals, but it may also be sourced from anthropogenic smelting factories and ore mines (Steinnes et al., 2000). Of those measured in this study, Fe and Al are the most likely to originate from a variety of sources as they are processed widely (Steinnes et al., 2000) and are common constituents in silicate-based dusts. Similarly, Zn may also be associated with biological material in addition to smelting emissions (Steinnes et al., 2000).

2.4.5 Biomass Tracers

This group was introduced out of necessity given the results obtained. The other classifications were somewhat expected from hypothesised local sources; however, this group was introduced to account for the high quantity of ~~potassium~~ K-based particles observed in one of the flights. These particles have negligible measurements of ~~silicon~~ Si and are not thought to be mineralogical in nature. This category has been dubbed "Biomass Tracers" as several studies (e.g. Andreae, 1983; Chou et al., 2008; Hand et al., 2010; Quennehen et al., 2012) have identified particles sourced from biomass burning events to be rich in this element. These K-rich particles have been found to be prominent in forest fire and anthropogenic combustion emissions~~, and may not be expected to be present~~ It is unlikely that such particles could be sourced in the Arctic, therefore their presence may infer transport from elsewhere ~~atmosphere~~ (Quennehen et al., 2012). Biomass burning produces particles known as bottom ashes, which differ from the fly ash particles that are typically emitted during fossil-fuel incomplete combustion processes (Umo et al., 2015). Activities which may produce these constituents could include firewood or agricultural burning (Andreae, 1983), or wildfires in warmer climates (Seiler and Crutzen, 1980).

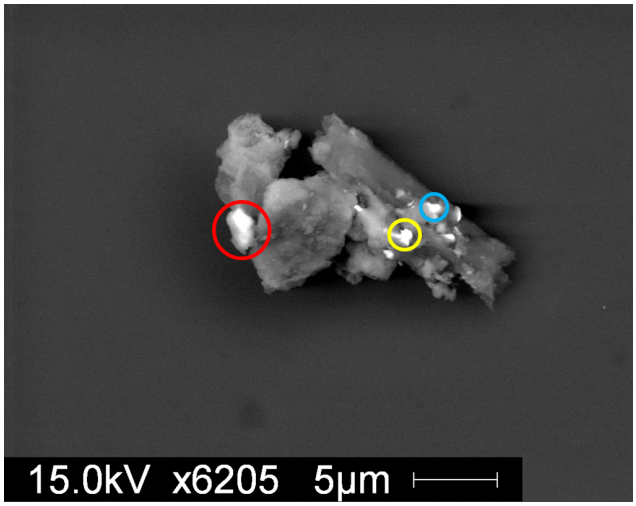

Figure 2: ~~Well-~~ Mixed particle from ~~B765~~ case 5. The circles denote the spots scanned to give the following dominating elements: Red – Fe, Si and Al; Yellow – Fe, Cr, Ni, Si and Al; Blue – Fe, Cr, Ca, Cl, S, Si and Al. Scan of full particle indicates Si dominance.

2.4.6 Other

This group contains particles which are not classified by the applied scheme. The implication is that these particles are ~~well-~~mixed. Figure 2 illustrates the difficulty with ~~internally-~~mixed particles; though local sites on the particle may be strongly influenced by certain elements, the SEM analysis does not provide a spatial map of the elemental distribution across each particle surface ~~automated scan will not catalogue the spatial dependencies and instead computes a mean spectra for presented particle surface area~~.

~~Internally-m~~ Mixed particles are typically either unclassified or classified by their most abundant elements ~~on average~~. The particle illustrated in Fig. 2 would be classified as a silicate dust since it is ~~well-~~mixed but has a dominating Si influence. The size of the samples prevent manual inspection of every ~~internally-mixed~~ unclassified particle, therefore the abundance of ~~well-~~mixed particles within a dataset must be inferred from the quantity quoted as "Other".

3 Results

3.1 HYSPLIT Back Trajectories

Air mass histories were calculated using HYSPLIT for each of the filter exposures to provide context with the environmental conditions in which they were sampled. Figure 3 shows the spatial extent of these trajectories in the top two panels and the mean altitudes covered are shown in the bottom panel.

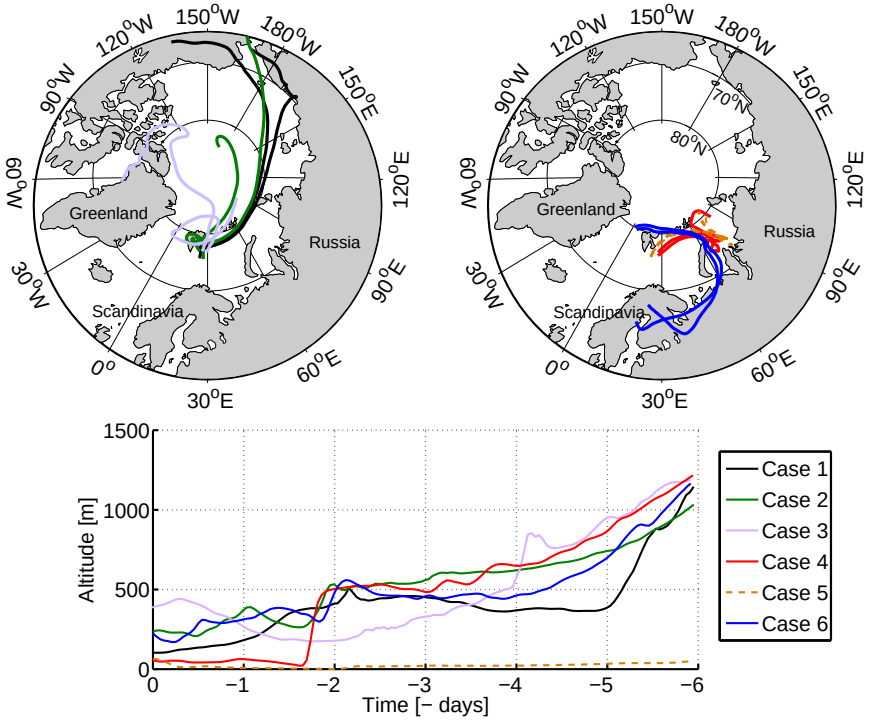

Figure 3: HYSPLIT air mass back trajectories for ~~each of the 6 exposures~~ cases 1–6, initialised at the aircraft's position and calculated 6 days backwards. Trajectories at the beginning and end of each exposure are shown. Top left panel: ~~B760~~ cases 1 (black), ~~B761~~ 2 (green) and ~~B762~~ 3(purple); top right panel: ~~B764~~ cases 4 (red), ~~B765~~ 5 (orange) and ~~B768~~ 6 (blue). The mean altitude covered by each of these trajectory groups is shown in the bottom panel.

The mean altitude of the trajectories remains within the lower 1.5km of the atmosphere. The modelled altitude typically increases ~~monotonically~~ with increased time backwards. ~~The case from B765~~ Case 5 is the exception to this trend, as consistent low-altitude trajectories are modelled for the full duration shown. Also, the majority of these trajectories are reasonably smooth; however, a significant descent in height is modelled in ~~the B764~~ case 4 at approximately -2 days.

A north-easterly wind was observed for cases ~~B760 to B762~~ 1 to 3, bringing air from over the dense Arctic sea-ice to the region of interest to the south-east of Svalbard. When extended back by 6 days, it becomes apparent that the history of the air sampled in each of these cases is quite different. From Fig. 3, ~~B760 and B761~~ cases 1 and 2 show some similarities, with the latter displaying more curvature anti-clockwise than the former. The trajectories from ~~the B762 exposure~~ case 3 are markedly distinct from these two, with cyclonic curvature around the immediate vicinity of Svalbard and Greenland.

There is a clear partition in the direction of the trajectories as the spring campaign progressed. The first three exposures had source regions to the north and west of the exposure locations, whilst the

latter three primarily sampled from the east. These latter trajectories also appear to be more compact than the first three cases (Fig. 3). The air from ~~B764 and B765~~ cases 4 and 5 is traced back across the northern coast of Russia whilst the ~~B768~~ trajectories from case 6 ~~split in two and~~ cover the northern coast~~, inland Siberia~~ of Russia and Scandinavia. A large portion of these trajectories are clustered towards the continent, suggesting a strong influence on this sample from this region.

These two trajectory groups can be dissected further; two specific pairs can be identified (~~B760 and B761; B764 and B765~~ cases 1 and 2; 4 and 5) which display similar paths, and ~~B762 and B768~~ cases 3 and 6 appear unique in comparison. Overall, there appears to be a clear shift in the source region of these boundary layer exposures as the campaign progresses; from over the dense Arctic sea ice, through Greenland and Northern Russia to the European continent.

3.2 Aerosol Size ~~and Morphology~~

To investigate any issues with inlet collection efficiency (see Sect. 2.2), size distributions ~~of the resultant filter pair analysis~~ from the filter data were constructed and compared with ~~those averaged~~ arithmetic means ~~from~~ of the wing-mounted ~~aircraft~~ probe~~s~~ data over each exposure period. The number size distribution was computed similarly to Chou et al. (2008); namely, the total number of particles detected in each scan was normalised by the area covered ~~by the scan~~ and ~~the~~ total volume of air sampled, then scaled to the full filter area. Figure 4 illustrates these comparisons for each below-cloud filter pair analysed. ~~Data from the PCASP, CAS-DPOL and CDP instruments were combined to give a single distribution for each case: the CAS-DPOL data were used between sizes 2 and 10μm, with PCASP data used below 2μm and CDP data used above 10μm.~~ Data from the PCASP, CAS-DPOL and CDP instruments are shown for comparison. These data use the standard scattering cross-sections for the aircraft probes and no refractive index corrections were applied due to the expected ~~well-~~mixed aerosol population.

The agreement ~~of~~ between the filter-derived ~~data with~~ and the probe data ~~is clearly~~ appears dependent on the conditions sampled. For example, ~~the B762 filter pair~~ case 3 was exposed during a section where cloud haze was encountered, whereas ~~the B765, B768 and B760~~ cases 1, 5 and 6 were cleanly exposed out of cloud. ~~The B761 and B764 c~~ Cases 2 and 4 ~~appeared to~~ sampled small amounts of cloud at the end of their exposures – at which point the probes measured some amount of cloud droplets and/or swollen aerosol particles – therefore the distribution derived from the external probes differs somewhat to the filter particle distribution. The mean RH values (Table 2) from each exposure were high (>90 %) and the disagreement between filter- and probe-data in Fig. 4 appears to correlate with these values. Case 1 displays good agreement under lower RH conditions, whilst cases 2, 3, 4 and 5 display poorer agreement under higher RH conditions. However, case 6 displays good agreement under relatively high RH, and the derived values are similar, therefore these trends could be circumstantial. The RH measure for case 3 is not trusted and is likely a consequence of condensation on the detection surface.

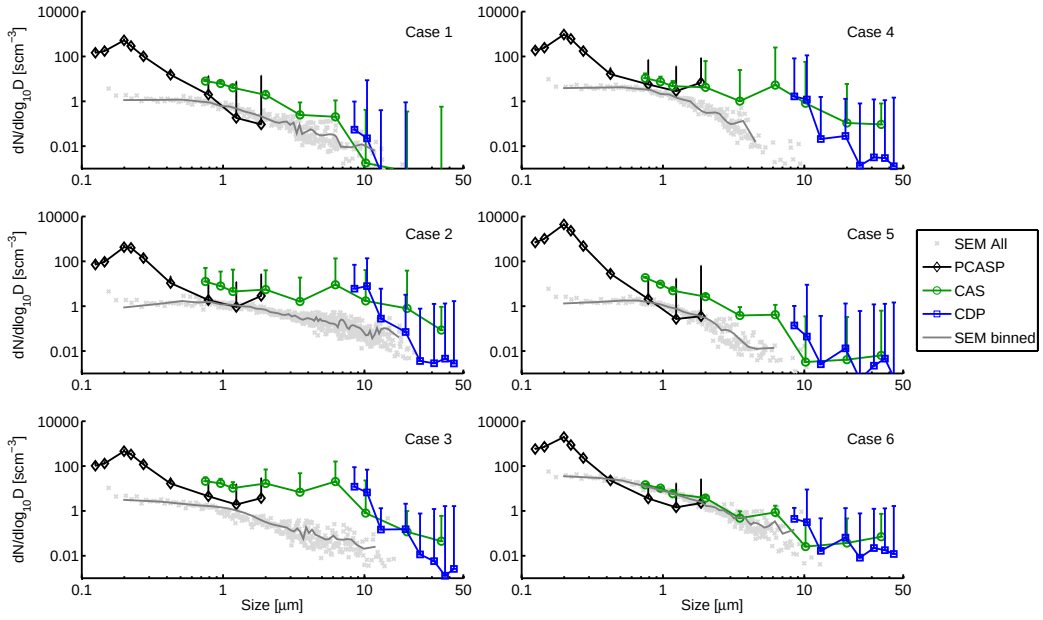

Figure 4: Size distributions ($\mathrm{dN/dlog_{10}D}$) of particle data obtained via ~~E~~SEM analysis compared with the averaged distributions derived from the optical particle counters at the relevant filter exposure times. ~~Red lines mark the 2 and 10μm thresholds where the probe data changes from PCASP to CAS-DPOL and from CAS-DPOL to CDP respectively. Probe data from cases B761, B762 and B764 show greater loadings at larger sizes due to some in-cloud sampling during the exposures; this heightens the likelihood that swollen aerosol particles and cloud droplets are measured by the externally-mounted CAS-DPOL and CDP.~~ PCASP, CAS and CDP data are shown in black (diamonds), green (circles) and blue (squares) respectively. Only upwards error bars are shown for clarity. SEM data are shown as scatter points (grey, crosses) and the arithmetic mean of these data is shown in dark grey.

Qualitatively, there is reasonable agreement between the probe and ~~E~~SEM-derived number size distributions – providing confidence in the analysis presented in this study – but this similarly highlights the limitations of the sample inlets on the aircraft for coarse aerosol as described by Trembath (2013). The discrepancies between these distributions, with relation to the inlet efficiency issues, are addressed further in Sect. 4.1.

3.3 Aerosol Composition

The particle classifications detailed in ~~Sect. 2.4~~ Table S1 were applied to the compositional data obtained for each analysed filter pair. ~~An element index was introduced which takes the ratio of the weight percentages measured for each element to the sum from all elements measured (excluding C~~

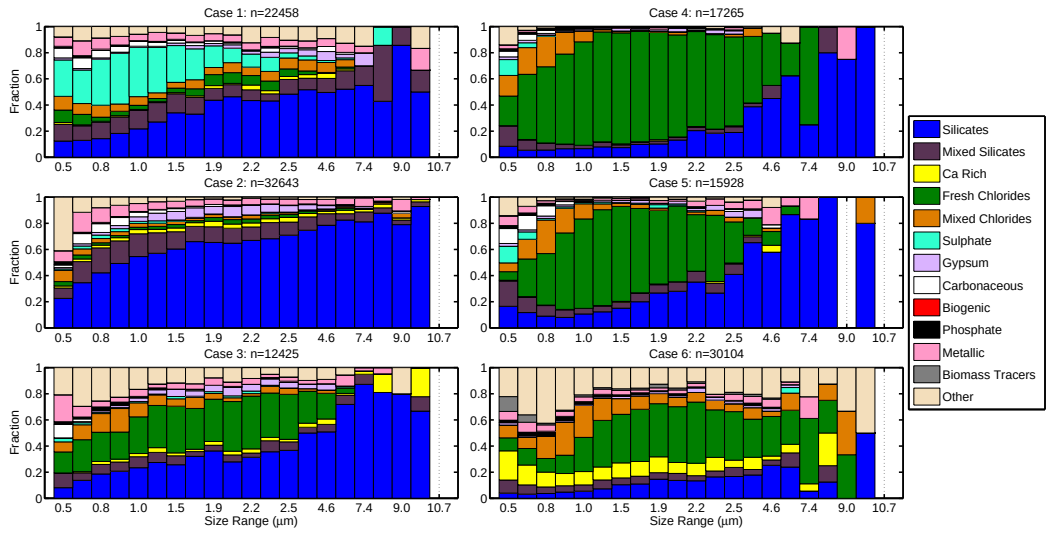

Figure 5: Size-segregated particle classifications applied to each below-cloud filter pair analysed from the considered flights, with each bin normalised to show the fraction (by number) occupied by each classification. The sizes indicated are the bin centres. The number of particles scanned in each case is listed at the top of each subfigure.

~~and O) for each particle, thus allowing the relationships between the elements of interest to be considered in isolation from the filter influence (Mamane and Noll, 1985;Kandler et al., 2007. Figure 5 displays the averaged classifications for each flight, split into sizes less than and greater than 0.5μm, and there is high variability in composition between each case. The contributions of metallic and mixed chloride particles are approximately independent of size; however, some categories display a clear dependence. For example, sulphates, carbonaceous and biomass tracers are detected strongly in the sub-micron range whilst silicates and fresh chlorides dominate the super-micron range.~~ The dependence of composition on size is ~~emphasised~~ shown in Fig. 5, where only ~~the~~ sizes which ~~show~~ display good agreement with the wing-mounted probes have been included ($\sim$0.5–$\sim$10 µm). Data outwith this range was viewed as being unrepresentative of the population, given the discrepancies at small and large sizes in Fig. 4. ~~Size-segregated compositional data for sizes smaller than this range have not been included as these may not be representative of the true conditions (see Fig. 4) and also have increased signal-to-noise issues from the measurement technique (Kandler et al. 2011).~~

Clear trends become apparent when implementing this size-segregated approach. In all samples, silicate-based dusts are identified, with greater concentrations ~~clearly~~ found at larger sizes for all cases except ~~B768~~ the last. The presence of these dusts is most abundant in the first three cases. ~~Filters from B764 and B765~~ Cases 4 and 5 are heavily dominated by fresh chlorides at all sizes except the largest bins, and ~~B762 and B768~~ cases 3 and 6 also have significant fractions of this species. ~~The~~

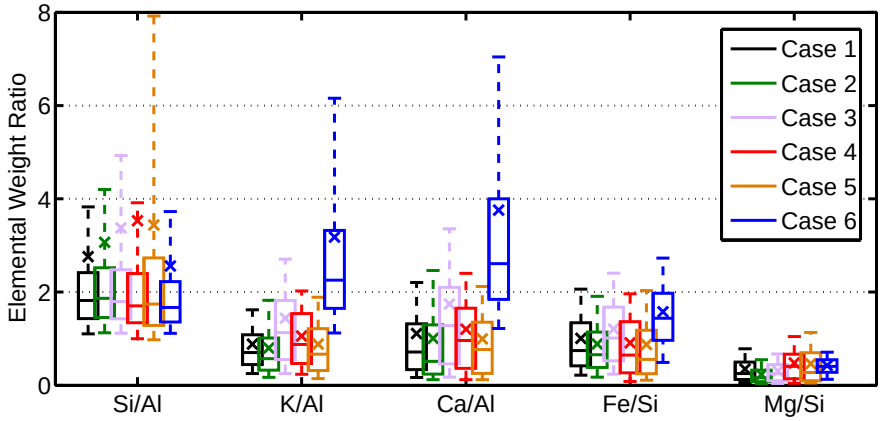

Figure 6: Mean elemental ratios from each flight. Only data from the silicates and mixed silicates categories are included to provide an indication of the mineral phases measured. The box edges indicate the 25th and 75th percentiles, and the cross and the horizontal line dissecting the boxes represent the mean and median values respectively. The outliers extend to the 10 and 90 % thresholds of the data.

~~B768 sample~~ Case 6 differs from the others, displaying increased Ca-rich, mixed chloride and other fractions. Similarly, the high sulphate loading in ~~B760~~ case 1 is ~~unlike the other cases~~ unique, yet the composition trends of this case can be associated with the subsequent flight via the abundance of silicates; a link that is not so clear between ~~B765 and B768~~ cases 5 and 6.

With regards to the mineral phase of the silicate dusts collected, elemental ratios can be used to identify trends. For example, feldspars can be rich in Ca, K or Na, whilst clays may have significant fractions of Mg and/or Fe. The elemental ratios displayed in Fig. 6 are variable across the campaign. This variability is heightened in some ratios with respect to others; from Fig. 6, ~~it is clear that~~ the K/Al and Ca/Al ratios are ~~is highly~~ changeable but the Mg/Si ratio is low for all cases. The mean and median values of the Si/Al ratio do not differ substantially between the flights~~; however, the mean value displays a clear peak during B764. The spread in the Si/Al ratio increases almost monotonically for the first five cases, with the maximum range displayed in B765~~. The K/Al, Fe/Si and Ca/Al ratios are ~~especially~~ heightened in ~~the B768 case~~ case 6, and show consistency across ~~each other case~~ the other cases with the exception of ~~B762~~ case 3. ~~A comparable trend is also evident with the Fe/Si ratio and the Mg/Si ratio is slightly raised for cases B764 and B765~~.

3.4 Comparison between Below and Above Cloud Samples

The samples detailed previously were all exposed below cloud and were chosen as the particles collected likely influenced the cloud microphysics of clouds that formed above these exposure altitudes. Most of these cases appear to be influenced by local sources; cases ~~B764 and B765~~ 4 and 5 in partic-

Table 4: Summary of sampling conditions during the two B764 exposures (cases 4 and 7). Values quoted are ~~averaged quantities~~ arithmetic means, with 1σ in brackets where appropriate.

Case	Position[a]	Conditions sampled	Exposure Length (s)	Volume of Air (sL)	Latitude (°N)	Longitude (°E)	Altitude (m)	Temperature (°C)	RH (%)
4	Below ~~cloud~~	Clear[b]	540	754.8	76.6	27.2	91 (86)	-9	97.4
7	Above ~~cloud~~	Clear	720	1080.2	76.4	27.1	833 (59)	-13	86.9

[a] With respect to the observed cloud layer.

[b] Some cloud base sampling was encountered at the end of the exposure.

ular are predominantly composed of fresh chlorides. However, these cases do not obviously address the involvement of aerosol particles from distant sources.

As a test case, a filter pair exposed above cloud was analysed to compare the particle compositions. A ~~case~~ comparison study was chosen: flight B764 provided consecutive filter exposures below and above (cases 4 and 7) a stratus cloud deck, approximately one hour apart, allowing a comparison between the respective compositional characteristics. The cloud located between the exposures was mixed-phase, with a sub-adiabatic CDP liquid-water content profile measured. This suggests that entrainment of aerosol from above may be an important source contributing to changes in the cloud microphysical properties in this case (Jackson et al., 2012), or that the liquid-water in the cloud has been depleted via precipitation processes. The air-mass back trajectories varied little between the exposures, with both cases influenced by air from over the Barents Sea and the coast of Northern Russia (see Fig. 3). The conditions sampled during each of these exposures are summarised in Table 4.

Figure 7 highlights the differences between the below and above cloud samples. The fraction of unclassified particles is greater in the above cloud example for sizes $> 0.5\,\mu m$ (panel B), whilst a similar fraction was observed in both cases for sizes $\leq 0.5\,\mu m$ (panel A). Similarly, a comparable fraction of silicates is found on both filter pairs. Greater fractions of fresh chlorides are found ~~on the below cloud sample~~ in case 4; however, a moderate loading of sea salt – and aged sea salt – is still identified in ~~the above cloud~~ case 7. The above cloud exposure also has a greater sulphate loading and the absolute number of particles detected was lower than in the below cloud case. The size-segregated classifications, shown in panel C of Fig. 7, display significant unclassified fractions across most sizes, with increased contributions at < 1 and $> 3\,\mu m$. The dominating species changes from unclassified to fresh chlorides to silicates as particle size increases and significant mixed chloride fractions were also observed at small sizes.

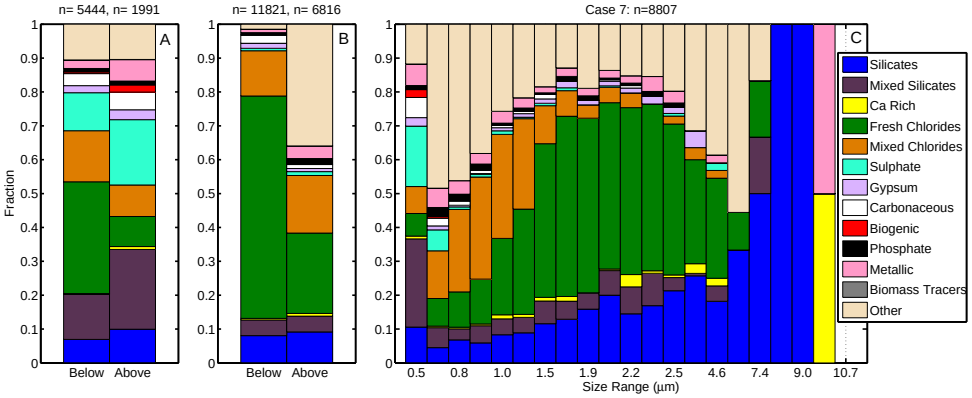

Figure 7: Compositional comparison between the below and above cloud samples (cases 4 and 7) from flight B764. Panel **(a)**: averaged particle classifications $\leq 0.5\,\mu$m; panel **(b)**: averaged particle classifications $>0.5\,\mu$m; panel **(c)**: Size-segregated classifications from the above cloud exposure. Each bin is normalised to show the fraction (by number) occupied by each classification, and the number of particles analysed are listed in panels **(a)** and **(b)**. The sizes indicated in panel **(c)** are the bin centres. The number of particles measured in each case are listed above each subfigure.

4 Discussion

4.1 ~~Case Overview~~ Size distributions

The filter-derived and probe-averaged size distributions from Sect. 3.2 compare reasonably well. The disagreement at the size limits ($\lesssim 0.5$ and $\gtrsim 10\,\mu$m) of these distributions implies that the inlet collection and filter efficiency issues ~~(e.g. from the sub-isokinetic sampling)~~ discussed in Sect. 2.2 are influencing these samples. These collection issues have been found to have the greatest impact on the coarse mode (Andreae et al. 2000; Formenti et al., 2003). The results shown in Fig. 4 reflect this, where the agreement between the filter- and probe-distributions decreases with increasing size ($\gtrsim$1-2 μm). Coarse-mode enhancement relative to the probe data is not observed to the same extent as Chou et al. (2008). Reasonable agreement between these data is observed up to approximately 10μm, as also concluded by Johnson et al. (2012), whose samples were analysed using the same facilities in the Williamson Research Centre, and Chou et al. (2008).

~~It is also probable that sub-micron particles either pass through the filter pores at the time of exposure or are left undetected by the EDS analysis due to a decreasing signal-to-noise ratio with decreasing particle size (Kandler et al. 2011). It is therefore concluded that the extremes of the particle size distribution collected by the filters and analysed by the ESEM/EDS system are under-represented. This is the same conclusion reached by Johnson et al. (2012) for their ESEM/EDS~~

~~comparison with airborne particle measurements, whose samples were analysed using the same facilities in the Williamson Research Centre.~~

Regarding the < 0.5 μm disagreement, it is possible that sub-micron particles either pass through the filter pores at the time of exposure or are left undetected by the EDS analysis due to a decreasing signal-to-noise ratio and increasing interaction volume with decreasing particle size (Kandler et al. 2011). ~~Similarly, the size characteristics of the aerosol particles collected by Chou et al. (2008) compared reasonably well – within a 1-σ confidence level – with measurements from optical particle counters mounted externally on their measurement aircraft. Crucially,~~ Chou et al. (2008) found that their accumulation-mode filter size distributions derived from Transmission Electron Microscopy (TEM) correlated better with observational data obtained from a cabin-based PCASP variation (CVI-PCASP) than their ~~E~~SEM-derived distributions. Given the similarity between the filtration techniques applied, this may suggest that the disagreement between the accumulation-mode distributions observed in this study could be a result of the limitations of the ~~E~~SEM technique rather than an issue with the filter sampling from the aircraft. However, Chou et al. (2008) also identified differences between the performance of their CVI-PCASP and externally-mounted PCASP – with the former consistently over-counting compared to the latter – suggesting that possible inlet losses could be similarly affecting the wing-mounted PCASP used in this study. In summary, the ~~E~~SEM technique, the filter mechanism collection efficiency and possible inlet losses could all be introducing some magnitude of error to the comparisons shown in Fig. 4, and it is not trivial to identify which source of error is the most influential in these cases.

4.1.1 Cases ~~B760 - B765~~ 1 to 5

The compositional trends observed in ~~Figs. 5 and~~ Fig. 5 are typically different between each ~~flight~~ case. Compositional dominance varies from sulphates to silicates to fresh chlorides through the first five cases. Some particle classes, e.g. carbonaceous or sulphates (excluding case 1), are mostly observed at sizes $<1\mu$m, whilst others (e.g. silicates) are more common at larger particle sizes.~~The difference between dominant classifications at sizes less than or greater than 0.5μm is clear (Fig. 5), and~~. Kandler et al. (2009) ~~observed a similar size dependence in their sample. They~~ also observed a distinct shift in average composition of particles at the 0.5 µm diameter limit, where the principal compositions in their African sample switched from sulphates to silicates and other minerals.

The influence of sulphates, silicates and fresh chlorides varies substantially in the first five ~~flights~~ cases; variability which could be inferred from the differences in the respective back trajectories. There are distinct similarities between the trends derived for ~~the B764 and B765~~ cases 4 and 5, with dominant fresh chloride and silicate signatures observed (Fig. 5). ~~Both cases also display a similar loading of mixed chlorides at sizes $> 0.5\mu$mm (Fig. 5)~~ Both cases display a similar mixed chloride loading between sizes 0.5μm and 1μm; particles which are likely sea salts mixed with sulphates.

The chloride classifications are not ubiquitously observed in the first five cases, with particularly low measurements of these species in ~~B760 and B761~~ cases 1 and 2. This suggests that the ocean was not a strong source of aerosol particles in these cases, whereas the significance of this source is clear in cases ~~B762, B764 and B765~~ 3, 4 and 5. This hypothesis is strengthened by the back trajectories calculated for these exposures (Fig. 3); the air-mass source for ~~the B760 and B761~~ cases 1 and 2 was the frozen Arctic Ocean, whilst cases ~~B764 and B765~~ 4 and 5 both had low-altitude trajectories across the sea surface. During the transition over the ocean, sea salts could have been lifted into the air stream. ~~The B760 c~~ Case 1 displays a high sulphates signature ~~at sub-micron sizes~~ – a characteristic unique from the other cases – suggesting that the particles had sufficient time to interact with sulphate gases (from either anthropogenic or marine sources, see Sect. 2.4.2) during transit over the ~~frozen Arctic Ocean~~ sea-ice. There is a common link between the first three cases in their respective silicate loadings; the measured amount of silicate-based dusts ~~was~~ is high in these cases, with a maximum reached during ~~B761~~ case 2.

4.1.2 Case ~~B768~~ 6

~~The B768 sample~~ Case 6 was ~~collected~~ exposed in a slightly different location – to the north-west of Svalbard instead of the south-east – than the first five cases (see Table 1). The particle loading was much greater for this case, as shown by the large number of particles collected (Fig. 5) and the very short sampling time (Table 2). ~~, as illustrated clearly by the filter-derived size distributions shown in Fig. 4~~. The comparatively greater number concentration measured agrees with the aerosol climatology presented by Tunved et al. (2013) and results from the ASTAR 2000 campaign (Hara et al. 2003), where trajectories from northern Russia and Europe coincided with noted "haze" events with an increased particle loading. Additionally, there are distinct compositional differences between ~~the first five cases and the B768 case~~ cases 1–5 and case 6. This case is the only one not to be dominated by silicates at super-micron sizes and ~~it was found to have~~ has the greatest proportion of Ca-rich particles, biomass tracers and unclassified particles across the sizes considered. ~~The B768 c~~ Case 6 is unique in its dominant particle categories, their respective size evolution and air mass back trajectory, emphasising its contrast to the other cases. ~~This is particularly clear with the sub-micron particles detected (Fig. 5).~~

The magnitude of the biomass tracer fraction ~~was~~ is only sufficient enough to be observed in ~~the B768~~ case 6. These particles are ~~more prevalent~~ mostly observed at small sizes, as seen in Fig. 5. Andreae (1983) have previously shown that there is a strong relationship between biomass particle species and particle size below 2 µm. The K measurements in these particles mirror the quantities measured by Umo et al. (2015) for bottom ashes, adding confidence to their identification as biomass products. The modelled back trajectory for ~~the B768~~ case 6 hailed from Northern Russia and the European continent. A potential source of these particles could be from similar boreal forest fire

events to those sampled by Quennehen et al. (2012), which was also observed at approximately the same time of year, or from European biomass activities.

The Ca-rich particles observed strongly in ~~B768~~ case 6 are distinct and not observed to the same magnitude in the other flights, implying a unique source. It is possible that these are naturally-occurring carbonate dusts; however, Umo et al. (2015) also measured several species of Ca-based dusts in their wood and bottom ash samples, suggesting that these could also be sourced from biomass burning activities. The strong detection of Ca-rich particles alongside the K-dominant biomass particles supports this conclusion in this case. The relative prevalence of K-rich and Ca-rich particles found in the sub- and super-micron ranges mirrors the relationship observed in the biomass burning study by Andreae (1983). The large Ca signature is also observed in the silicate and mixed silicate spectra for this case (Fig. S2 in the Supplement), and consequently affects the K/Al and Ca/Al ratios (shown in Fig. 6). It is unclear whether these enhanced values are a result of internal mixing of some silicates with the Ca- or K-rich biomass particles or if they are real feldspar signatures (as K-feldspar or plagioclase). The Fe/Si ratio is also elevated for this case and this could be due to increased detection of clay-like dusts or Hematite, and/or internal mixing with anthropogenic smelting emissions.

4.2 Sourcing the Dust

Unexpectedly, large fractions of silicate dusts ~~were~~ are observed – to different extents – in every case. These filters were collected in March when the majority of the surrounding surface was snow-covered, therefore there is no obvious local source of mineral dust. Weinbruch et al. (2012) also identified large dust fractions in their samples collected at Ny Ålesund in April 2008, and these dusts would likely act as a source of ice nucleating particles for clouds in this region. The presence of dust in such quantities could either be due to some local source, long-range transport or a combination of these two avenues. To better understand the characteristics of these dusts, the elemental ratios in Fig. 6 can be considered. In general, the consistency in the median Si/Al ratio between each case suggests that the typical composition of the aluminosilicates has low variability, with each distribution skewed differently to account for the differences in the mean and variance values.

Elemental ratios can be used to infer a source of the mineral dusts, and several studies have investigated characteristic ratios of dusts from a variety of arid regions. For example, the African dust study by Formenti et al. (2008) calculated these ratios from airborne filter data and derived Si/Al, K/Al and Ca/Al ratios of approximately 3, 0.25 and 0.5 respectively. These values are within the limits of those calculated in this study (Fig. 6); however, a lack of good agreement suggests that these sources may not be related to the dusts analysed here. Zhang et al. (2001) presented these ratios for dusts collected at various Asian sites, and their Tibetan and Loess Plateau samples were found to have Si/Al ratios of 4.6 and 2.5 respectively. The Loess values are ~~more~~ consistent with the mean values obtained ~~from B760, B761 and B768~~ in all cases, whereas the Tibetan values lie

within the upper bounds of samples ~~B762, B764 and B765~~ 3 and 5. The Loess samples also had a Ca/Al ratio of 2.7, which lies between the median and mean values obtained for ~~B768~~ case 6, and is within the upper bound of ~~B762~~ case 3; however, it is much greater than the average ratio derived for the majority of the cases presented. The K/Al ratio was found to be 0.95, consistent with the first five cases but not ~~B768~~ case 6. This could be due to the heightened K influence from biomass sources in ~~B768~~ case 6 ~~from biomass sources~~, but could also be coincidental and care must be taken when attributing a transported dust sample to a given source via this method. The dust collected by the aircraft filters during ACCACIA does appear to have more in common with the Asian samples than the African samples; however, the composition of dusts originating from the same source region is not always consistent and can vary quite substantially between close geographical locations (Glen and Brooks, 2013). It is also unclear how these ratios would be affected by transportation, as atmospheric processing ~~will~~ would likely alter the composition of ageing dust with respect to the freshly-emitted dust samples ~~mentioned here~~ presented in these studies. Despite this, it is worth noting that Liu et al. (2015) identified high-altitude plumes during the springtime ACCACIA campaign which hailed from the Asian continent. It could be possible that dusts from these sources were advected over large distances in addition to the black carbon explicitly measured and modelled by Liu et al. (2015). The increase in mean trajectory altitude with time, as shown in Fig. 3, supports this theory as the descent of air from > 1000 m could be drawing dusts down to the low-altitudes considered. The theory that Asian dust contributes to the Arctic Haze is not new, and some observations indicate that this is the case (e.g. Rahn et al., 1977), yet models have not been able to produce conclusive evidence (Quinn et al., 2007). A key question in this hypothesis is theorising how the dust ~~travels~~ is lofted up to high altitudes in the atmosphere, and subsequently undergoes this long-range transportation, without experiencing cloud processing. It is possible that frontal uplifts at the source are responsible, with weakly-scavenging mixed-phase clouds along the trajectories allowing the dust loading to remain so high.

4.3 ~~Internally-~~Mixed Aerosol Particles

The degree of ~~internal~~ mixing in each case is different – as displayed by the variability in mean fractions shown in Fig. S2 in the Supplement – thus tying in with the differences between the air mass histories. Particles which have undergone long-range transport likely would have enhanced internal mixing and may not be adequately classified by the scheme employed in this study. Unclassified particles are prevalent in ~~the B761, B762 and B768 below-cloud~~ cases 3, 6 and 7 (Fig. 5). The variability within the categories (as seen in Fig. S2 in the Supplement) highlights the importance of treating the classifications with caution: they provide a good representation of the particle species collected, yet the ability of the ~~classification~~ criteria to accurately account for ~~internally-~~mixed species is not always efficient. The extent of the unclassified category must always be considered to account for this.

The influence of ~~internally-mixed, transported~~ mixed particles on the population is most evident from the higher-altitude case: ~~the B764 above-cloud sample~~ case 7 ~~detailed in~~ (Fig. 7) is distinctly different from its below-cloud counterpart (case 4, Fig. 5). In addition to the enhanced other fraction, large mixed chloride, sulphate and mixed silicate loadings were also identified above cloud (Fig. 7); classifications which could be attributed to anthropogenic influences. In this case, it is likely that these particles had undergone mixing over long-range transport. The contrast between the below and above cloud cases emphasises the segregation of the Arctic aerosol sources: whilst being influenced by local surface sources, the Arctic atmosphere is also affected by this influx of long-range transported aerosol particles – the Arctic Haze – during the spring months (Barrie, 1986; Shaw, 1995; Liu et al., 2015). Both of these aerosol pathways will affect the cloud microphysics, and further investigation is required to better understand the importance of each. The particle classes detected in cases 4 and 7 could have interacted with the cloud layer as CCN or INPS, whilst the differences between them can be explained by the cloud restricting any direct mixing between the two populations.

~~The differences in composition between the below and above cloud samples can be explained by the presence of the cloud in between: the particles present would have interacted with the cloud as CCN or INPs, and so the cloud inhibited the direct mixing of these two aerosol populations. This could have unclear consequences for the resultant cloud microphysics as internally-mixed particles (e.g. with some mineral constituent) could act as INPs or (Giant) CCN dependent on the mixing state and the hygroscopicity of the particle (see Sect. 2.4.3). A complex particle is difficult to clearly categorise as an INP or CCN as its nucleation will be heavily dependent on the environmental conditions. The presence of coatings on particles can also have a significant impact on their role in aerosol-cloud interactions. Coatings of soluble material could enhance CCN ability and promote secondary ice production via the formation of large cloud drops (Levin et al. 1996), whilst organic coatings could suppress the nucleating ability of an efficient INP (Möhler et al., 2008).~~

The ~~complexity~~ extent of internal and external mixing observed indicates that some INP predictions may be fraught with inaccuracy in this region; for example, DeMott et al. (2010) relate INP concentration to the total aerosol concentration $> 0.5\,\mu m$ under the assumption that most of the particles in this limit are INPs. However, efficient INPs (e.g. mineral dusts) were not found to be consistently dominant in this study. As suggested by DeMott et al. (2010), this relation may not be applicable in cases heavily influenced by marine sources, and the high loadings of super-micron sea salt identified in some of the ACCACIA cases would qualify these as such. The use of dust-based parameterisations such as Niemand et al. (2012) or DeMott et al. (2015) may provide a more accurate prediction of the INP concentration in these cases. ~~Despite this, the ice nucleating ability of the unclassified and mixed particle categories is not quantifiable in this study and it is likely that they would,~~

Whilst it is likely that the dusts observed in this study would act as INPs, it cannot be determined how the unclassified and mixed particle categories would interact with the clouds in this region.

In particular, the lack of sound quantitative C and O measurements prevents organic coatings from being identified; coatings which are important in interpreting aerosol-cloud interactions. The mixed particles identified here could likely act as CCN as they would possess a soluble component provided by the Cl or S signatures. However, it is also likely that they could influence the INP population; whilst soluble coatings may suppress ice nucleating ability, the presence of IN-active coatings and/or complex internal-mixing could act to enhance it. Examples of IN-active coatings could include biological material, as some strains of bacteria have been observed to be efficient INPs in laboratory studies (Möhler et al., 2007; Hoose and Möhler, 2012). Some studies have identified cases where bacteria has survived long-range atmospheric transport by piggybacking dust particles (Yamaguchi et al., 2012). It is possible that such bacteria could influence the Arctic atmosphere via a similar transportation mechanism. Fundamentally, comprehending how these mixed particles interact and impact the cloud microphysics is a significant step to take towards improving our understanding of aerosol-cloud interactions in the Arctic springtime.

5 Conclusions

During the Aerosol-Cloud Coupling and Climate Interactions (ACCACIA) springtime campaign, in-situ samples of Arctic aerosol particles were collected on polycarbonate filters. Analysis of these samples has been detailed, with a focus placed upon identifying the composition of the collected particles and investigating their potential sources. In total, six below-cloud exposures were analysed to infer how the local sources may influence the cloud microphysics of the region (Fig. 1)~~. Additionally,~~ and one above-cloud filter pair was analysed to investigate the composition of transported particles (Fig. 7). The main findings of this study are as follows:

- Single-particle analysis of the filters produced number size distributions which were comparable (over sizes $\sim$0.5–$\sim$10 μm) to those derived from the wing-mounted optical particle counters (Fig. 4). Better agreement between these distributions was achieved in lower RH sampling conditions. The composition of the particles collected was strongly dependent upon size across all samples, with crustal minerals and sea salts dominating the super-micron range. Carbon- and sulphur-based particles were ~~prevalent~~ mostly observed in the $<$ ~~0.5~~1 µm limit ~~(Fig. 5~~(Fig. 5). Large fractions of ~~complex internal mixtures~~ mixed particles – as shown by the other, mixed silicate and mixed chloride categories in Fig. 5 – were identified in each case ~~as expected~~. The impact of these particles on cloud microphysics as potential INPs and/or CCN is not quantifiable by this study~~; however, it is likely that the silicate dusts identified would act as a source of INPs for clouds in this region.~~

- ~~There are d~~ Distinct size-dependent compositional trends were observed in each sample, with stark differences between cases (Fig. 5). These differences were attributed to variations in the air mass histories; cases ~~B760 and B761~~ 1 and 2 presented a ~~clear~~ silicate dust dominance ~~and~~

~~the B764 and B765~~ whilst cases 4 and 5 ~~were found to have very~~ had similar chloride and silicate ~~abundances~~ loadings. These similarities were mirrored by their closely-related source regions (Fig. 3). The relationship between composition and trajectory was strengthened by the unique attributes of ~~the B768~~ case 6; both the trends and trajectory were distinct in this case and the particle classifications identified can be explained by hypothesised sources along the trajectory presented.

– Crustal minerals were identified in all cases, despite the seasonal local snow cover. The HYSPLIT back trajectories (Fig. 3) were variable in direction, yet typically increased in mean altitude over time. Therefore, these dusts were hypothesised to have undergone long-range, high-altitude transport from distant sources, through regions containing weakly-scavenging mixed-phase clouds. Some elemental characteristics (Fig. 6) were found to be consistent with Asian dust sources; however, it is not known how long-range transport may affect the composition of these dusts and so this theory cannot be proven with this data.

The coarse-mode, non-volatile Arctic aerosol particles analysed by this study showed great variation between subsequent days and different meteorological conditions, therefore it would be difficult to incorporate these findings into models. However, the measurements from the springtime ACCACIA campaign provide a good opportunity to simultaneously investigate both the properties of aerosol particles in the region and the microphysical characteristics of the clouds observed. Further study of the cloud microphysics of these cases, with reference to these aerosol observations, will allow us to improve the representation of aerosol-cloud interactions in climate models and act to reduce the uncertainty in forecasting the Arctic atmosphere in the future.

Acknowledgements. This work was funded by the National Environment Research Council (NERC), under grant NE/I028696/1, as part of the ACCACIA campaign. G. Young was supported by a NERC PhD studentship. We would like to thank the ACCACIA project team for their efforts, and J. Crosier and N. Marsden for their helpful comments and advice. Airborne data were obtained using the BAe-146-301 Atmospheric Research Aircraft [ARA] flown by Directflight Ltd and managed by the Facility for Airborne Atmospheric Measurements [FAAM], which is a joint entity of the Natural Environment Research Council [NERC] and the Met Office. G. Young would also like to thank J. Fellowes and J. Waters at the Williamson Research Centre for their guidance with the ESEM instrument and the European Geosciences Union for funding the publication this article as part of an OSP 2015 award.

References

Andreae, M. O.: Soot Carbon and Excess Fine Potassium: Long-Range Transport of Combustion-Derived Aerosols, Science, 220, 1148–1151, doi:10.1126/science.220.4602.1148, 1983.

Andreae, M. O. and Rosenfeld, D.: Aerosol cloud precipitation interactions. Part 1. The nature and sources of cloud-active aerosols, Earth Sci. Rev., 89, 13–41, doi:10.1016/j.earscirev.2008.03.001, 2008.

Andreae, M. O., Elbert, W., Gabriel, R., Johnson, D. W., Osborne, S., and Wood, R.: Soluble ion chemistry of the atmospheric aerosol and SO concentrations over the eastern North Atlantic during ACE-2, Tellus B, 52, 1066–1087, doi:10.1034/j.1600-0889.2000.00105.x, 2000.

Barrie, L. A.: Arctic Air Chemistry: An Overview, in: Arctic Air Pollution, edited by: Stonehouse, B., Cambridge University Press, Cambridge, UK, 1986.

Behrenfeldt, U., Krejci, R., Ström, J., and Stohl, A.: Chemical properties of Arctic aerosol particles collected at the Zeppelin station during the aerosol transition period in May and June of 2004, Tellus B, 60, 405–415, doi:10.1111/j.1600-0889.2008.00349.x, 2008.

Chou, C., Formenti, P., Maille, M., Ausset, P., Helas, G., Harrison, M., and Osborne, S.: Size distribution, shape, and composition of mineral dust aerosols collected during the African Monsoon Multidisciplinary Analysis Special Observation Period 0: Dust and Biomass-Burning Experiment field campaign in Niger, January 2006, J. Geophys. Res., 113, D00C10, doi:10.1029/2008JD009897, 2008.

Connolly, P. J., Möhler, O., Field, P. R., Saathoff, H., Burgess, R., Choularton, T., and Gallagher, M.: Studies of heterogeneous freezing by three different desert dust samples, Atmos. Chem. Phys., 9, 2805–2824, doi:10.5194/acp-9-2805-2009, 2009.

Conny, J. M. and Norris, G. A.: Scanning Electron Microanalysis and Analytical Challenges of Mapping Elements in Urban Atmospheric Particles, Environ. Sci. Technol., 45, 7380–7386, doi:10.1021/es2009049, 2011.

Crosier, J., Allan, J. D., Coe, H., Bower, K. N., Formenti, P., and Williams, P. I.: Chemical composition of summertime aerosol in the Po Valley (Italy), northern Adriatic and Black Sea, Q. J. Roy. Meteor. Soc., 133, 61–75, doi:10.1002/qj.88, 2007.

Curry, J. A., Rossow, W. B., Randall, D., and Schramm, J. L.: Overview of Arctic Cloud and Radiation Characteristics., J. Climate, 9, 1731–1764, doi:10.1175/1520-0442(1996)009<1731:OOACAR>2.0.CO;2, 1996.

de Boer, G., Shupe, M. D., Caldwell, P. M., Bauer, S. E., Persson, O., Boyle, J. S., Kelley, M., Klein, S. A., and Tjernström, M.: Near-surface meteorology during the Arctic Summer Cloud Ocean Study (ASCOS): evaluation of reanalyses and global climate models, Atmos. Chem. Phys., 14, 427–445, doi:10.5194/acp-14-427-2014, 2014.

DeMott, P. J., Prenni, A. J., Liu, X., Kreidenweis, S. M., Petters, M. D., Twohy, C. H., Richardson, M. S., Eidhammer, T., and Rogers, D. C.: Predicting global atmospheric ice nuclei distributions and their impacts on climate, P. Natl. Acad. Sci. USA, 107, 11217–11222, doi:10.1073/pnas.0910818107, 2010.

DeMott, P. J., Prenni, A. J., McMeeking, G. R., Sullivan, R. C., Petters, M. D., Tobo, Y., Niemand, M., Möhler, O., Snider, J. R., Wang, Z., and Kreidenweis, S. M.: Integrating laboratory and field data to quantify the immersion freezing ice nucleation activity of mineral dust particles, Atmos. Chem. Phys., 15, 393–409, doi:10.5194/acp-15-393-2015, 2015.

Draxler, R. R. and Hess, G. D.: An Overview of the HYSPLIT_4 Modelling System for Trajectories, Dispersion, and Deposition, Aust. Meteorol. Mag., 47, 295–308, 1998.

Fleming, Z. L., Monks, P. S., and Manning, A. J.: Review: Untangling the influence of air-mass history in interpreting observed atmospheric composition, Atmos. Res., 104, 1–39, doi:10.1016/j.atmosres.2011.09.009, 2012.

Formenti, P., Elbert, W., Maenhaut, W., Haywood, J., Osborne, S. and Andreae, M. O.: Inorganic and carbonaceous aerosols during the Southern African Regional Science Initiative (SAFARI 2000) experiment: Chemical characteristics, physical properties, and emission data for smoke from African biomass burning, J. Geophys. Res., 108, 8488, doi:10.1029/2002JD002408, 2003.

Formenti, P., Rajot, J. L., Desboeufs, K., Caquineau, S., Chevaillier, S., Nava, S., Gaudichet, A., Journet, E., Triquet, S., Alfaro, S., Chiari, M., Haywood, J., Coe, H., and Highwood, E.: Regional variability of the composition of mineral dust from western Africa: Results from the AMMA SOP0/DABEX and DODO field campaigns, J. Geophys. Res., 113, D00C13, doi:10.1029/2008JD009903, 2008.

Formenti, P., Schütz, L., Balkanski, Y., Desboeufs, K., Ebert, M., Kandler, K., Petzold, A., Scheuvens, D., Weinbruch, S., and Zhang, D.: Recent progress in understanding physical and chemical properties of African and Asian mineral dust, Atmos. Chem. Phys., 11, 8231–8256, doi:10.5194/acp-11-8231-2011, 2011.

Geng, H., Ryu, J., Jung, H.-J., Chung, H., Ahn, K.-H., and Ro, C.-U.: Single-Particle Characterization of Summertime Arctic Aerosols Collected at Ny-Ålesund, Svalbard, Environ. Sci. Technol., 44, 2348–2353, doi:10.1021/es903268j, 2010.

Glen, A. and Brooks, S. D.: A new method for measuring optical scattering properties of atmospherically relevant dusts using the Cloud and Aerosol Spectrometer with Polarization (CASPOL), Atmos. Chem. Phys., 13, 1345–1356, doi:10.5194/acp-13-1345-2013, 2013.

Hand, V. L., Capes, G., Vaughan, D. J., Formenti, P., Haywood, J. M., and Coe, H.: Evidence of internal mixing of African dust and biomass burning particles by individual particle analysis using electron beam techniques, J. Geophys. Res., 115, D13301, doi:10.1029/2009JD012938, 2010.

Hara, K., Yamagata, S., Yamanouchi, T., Sato, K., Herber, A., Iwasaka, Y., Nagatani, M. and Nakata, H.: Mixing states of individual aerosol particles in spring Arctic troposphere during ASTAR 2000 campaign, J. Geophys. Res., 108, 4209, doi:10.1029/2002JD002513, 2003.

Heintzenberg, J., Hansson, H.-C., Ogren, J. A., Covert, D. S., Blanchet, J.-P.: Physical and Chemical Properties of Arctic Aerosols and Clouds, in: Arctic Air Pollution, edited by: Stonehouse, B., Cambridge University Press, Cambridge, UK, 1986.

Hoose, C. and Möhler, O.: Heterogeneous ice nucleation on atmospheric aerosols: a review of results from laboratory experiments, Atmos. Chem. Phys., 12, 9817–9854, doi:10.5194/acp-12-9817-2012, 2012.

IPCC AR5: Clouds and Aerosols, in: Climate Change 2013: The Physical Science Basis, Contribution of Working Group I to the Fifth Assessment Report of the Intergovernmental Panel on Climate Change, edited by: Boucher, O., Randall, D., Artaxo, P., Bretherton, C., Feingold, G., Forser, P., Kerminen, V. M., Kondo, Y., Liao, H., Lohmann, U., Rasch, P., Satheesh, S. K., Sherwood, S., Stevens, B., Zhang, X. Y., and (Stocker, T. F., Qin, D., Plattner, G. K., Tignor, M., Allen,S. K., Boschung, J., Nauels, A., Xia, Y., Bex, V., and Midley, P. M., Cambridge University Press, Cambridge, United Kingdom and New York, NY, USA, doi:10.1017/CBO9781107415324.016, 2013.

Jackson, R. C., McFarquhar, G. M., Korolev, A. V., Earle, M. E., Liu, P. S. K., Lawson, R. P., Brooks, S., Wolde, M., Laskin, A., and Freer, M.: The dependence of ice microphysics on aerosol concentration in arctic mixed-phase stratus clouds during ISDAC and M-PACE, J. Geophys. Res., 117, D15207, doi:10.1029/2012JD017668, 2012.

John, W., Hering, S., Reischl, G., Sasaki, G., and Goren, S.: Characteristics of Nuclepore filters with large pore size – II. Filtration properties, Atmos. Environ., 17, 373–382, doi:10.1016/0004-6981(83)90054-9, 1983.

Johnson, B., Turnbull, K., Brown, P., Burgess, R., Dorsey, J., Baran, A. J., Webster, H., Haywood, J., Cotton, R., Ulanowski, Z., Hesse, E., Woolley, A., and Rosenberg, P.: In situ observations of volcanic ash clouds from the FAAM aircraft during the eruption of Eyjafjallajökull in 2010, J. Geophys. Res., 117, D00U24, doi:10.1029/2011JD016760, 2012.

Kandler, K., Benker, N., Bundke, U., Cuevas, E., Ebert, M., Knippertz, P., Rodríguez, S., Schütz, L., and Weinbruch, S.: Chemical composition and complex refractive index of Saharan Mineral Dust at Izaña, Tenerife (Spain) derived by electron microscopy, Atmos. Environ., 41, 8058–8074, doi:10.1016/j.atmosenv.2007.06.047, 2007.

Kandler, K., Schütz, L., Deutscher, C., Ebert, M., Hofmann, H., Jäckel, S., Jaenicke, R., Knippertz, P., Lieke, K., Massling, A., Petzold, A., Schladitz, A., Weinzierl, B., Wiedensohler, A., Zorn, S., and Weinbruch, S.: Size distribution, mass concentration, chemical and mineralogical composition and derived optical parameters of the boundary layer aerosol at Tinfou, Morocco, during SAMUM 2006, Tellus B, 61, 32–50, doi:10.1111/j.1600-0889.2008.00385.x, 2009.

Kandler, K., Lieke, K., Benker, N., Emmel, C., Küpper, M., Müller-Ebert, D., Ebert, M., Scheuvens, D., Schladitz, A., Schütz, L., and Weinbruch, S.: Electron microscopy of particles collected at Praia, Cape Verde, during the Saharan Mineral Dust Experiment: particle chemistry, shape, mixing state and complex refractive index, Tellus B, 63, 475–496, doi:10.1111/j.1600-0889.2011.00550.x, 2011.

Kanji, Z. A., Welti, A., Chou, C., Stetzer, O., and Lohmann, U.: Laboratory studies of immersion and deposition mode ice nucleation of ozone aged mineral dust particles, Atmos. Chem. Phys., 13, 9097–9118, doi:10.5194/acp-13-9097-2013, 2013.

Krejci, R., Ström, J., de Reus, M., and Sahle, W.: Single particle analysis of the accumulation mode aerosol over the northeast Amazonian tropical rain forest, Surinam, South America, Atmos. Chem. Phys., 5, 3331–3344, doi:10.5194/acp-5-3331-2005, 2005.

Krueger, B. J., Grassian, V. H., Laskin, A., and Cowin, J. P.: The transformation of solid atmospheric particles into liquid droplets through heterogeneous chemistry: Laboratory insights into the processing of calcium containing mineral dust aerosol in the troposphere, Geophys. Res. Lett., 30, 1148, doi:10.1029/2002GL016563, 2003.

Lance, S., Brock, C. A., Rogers, D., and Gordon, J. A.: Water droplet calibration of the Cloud Droplet Probe (CDP) and in-flight performance in liquid, ice and mixed-phase clouds during ARCPAC, Atmos. Meas. Tech., 3, 1683–1706, doi:10.5194/amt-3-1683-2010, 2010.

Levin, Z., Ganor, E., and Gladstein, V.: The Effects of Desert Particles Coated with Sulfate on Rain Formation in the Eastern Mediterranean., J. Appl. Meteorol., 35, 1511–1523, doi:10.1175/1520-0450(1996)035<1511:TEODPC>2.0.CO;2, 1996.

Levin, Z., Teller, A., Ganor, E., and Yin, Y.: On the interactions of mineral dust, sea-salt particles, and clouds: A measurement and modeling study from the Mediterranean Israeli Dust Experiment campaign, J. Geophys. Res., 110, D20202, doi:10.1029/2005JD005810, 2005.

Li, J., Pósfai, M., Hobbs, P. V., and Buseck, P. R.: Individual aerosol particles from biomass burning in southern Africa: 2, Compositions and aging of inorganic particles, J. Geophys. Res., 108, 8484, doi:10.1029/2002JD002310, 2003.

Liu, B. Y. H. and K. W. Lee: Efficiency of membrane and nuclepore filters for submicrometer aerosols, Environ. Sci. Technol., 10, 345–350, doi:10.1021/es60115a002, 1976.

Liu, D., Quennehen, B., Darbyshire, E., Allan, J. D., Williams, P. I., Taylor, J. W., Bauguitte, S. J.-B., Flynn, M. J., Lowe, D., Gallagher, M. W., Bower, K. N., Choularton, T. W., and Coe, H.: The importance of Asia as a source of black carbon to the European Arctic during springtime 2013, Atmos. Chem. Phys., 15, 11537–11555, doi:10.5194/acp-15-11537-2015, 2015.

Lloyd, G., Choularton, T. W., Bower, K. N., Crosier, J., Jones, H., Dorsey, J. R., Gallagher, M. W., Connolly, P., Kirchgaessner, A. C. R., and Lachlan-Cope, T.: Observations and comparisons of cloud microphysical properties in spring and summertime Arctic stratocumulus clouds during the ACCACIA campaign, Atmos. Chem. Phys., 15, 3719–3737, doi:10.5194/acp-15-3719-2015, 2015.

Mamane, Y. and Noll, K. E.: Characterization of large particles at a rural site in the eastern United States: Mass distribution and individual particle analysis, Atmos. Environ., 19, 611–622, doi:10.1016/0004-6981(85)90040-X, 1985.

Möhler, O., DeMott, P. J., Vali, G., and Levin, Z.: Microbiology and atmospheric processes: the role of biological particles in cloud physics, Biogeosciences, 4, 1059–1071, doi:10.5194/bg-4-1059-2007, 2007.

Möhler, O., Benz, S., Saathoff, H., Schnaiter, M., Wagner, R., Schneider, J., Walter, S., Ebert, V., and Wagner, S.: The effect of organic coating on the heterogeneous ice nucleation efficiency of mineral dust aerosols, Environ. Res. Lett., 3, 025007, doi:10.1088/1748-9326/3/2/025007, 2008.

Murray, B. J., O'Sullivan, D., Atkinson, J. D., and Webb, M. E.: Ice nucleation by particles immersed in supercooled cloud droplets., Chem. Soc. Rev., 41, 6519–6554, doi:10.1039/c2cs35200a, 2012.

Niemand, M., Möhler, O., Vogel, B., Vogel, H., Hoose, C., Connolly, P., Klein, H., Bingemer, H., DeMott, P., Skrotzki, J., and Leisner, T.: A Particle-Surface-Area-Based Parameterization of Immersion Freezing on Desert Dust Particles, J. Atmos. Sci., 69, 3077–3092, doi:10.1175/JAS-D-11-0249.1, 2012.

Perovich, D. K., Richter-Menge, J. A., Jones, K. F., and Light, B.: Sunlight, water, and ice: Extreme Arctic sea ice melt during the summer of 2007, Geophys. Res. Lett., 35, L11501, doi:10.1029/2008GL034007, 2008.

Pruppacher, H. R. and Klett, J. D.: Microphysics of Clouds and Precipitation, 2nd ed., Kluwer Academic Publishers, Dordrecht, the Netherlands, 1997.

Quennehen, B., Schwarzenboeck, A., Matsuki, A., Burkhart, J. F., Stohl, A., Ancellet, G., and Law, K. S.: Anthropogenic and forest fire pollution aerosol transported to the Arctic: observations from the POLARCAT-France spring campaign, Atmos. Chem. Phys., 12, 6437–6454, doi:10.5194/acp-12-6437-2012, 2012.

Quinn, P. K., Shaw, G., Andrews, E., Dutton, E. G., Ruoho-Airola, T., and Gong, S. L.: Arctic haze: current trends and knowledge gaps, Tellus B, 59, 99–114, doi:10.1111/j.1600-0889.2006.00238.x, 2007.

Rahn, K. A.: Relative importances of North America and Eurasia as sources of arctic aerosol, Atmos. Environ., 15, 1447–1455, doi:10.1016/0004-6981(81)90351-6, 1981.

Rahn, K. A., Borys, R. D., and Shaw, G. E.: The Asian source of Arctic haze bands, Nature, 268, 713–715, doi:10.1038/268713a0, 1977.

Reimann, C., Banks, D., and Caritat, P. D.: Impacts of Airborne Contamination on Regional Soil and Water Quality: The Kola Peninsula, Russia, Environ. Sci. Technol., 34, 2727–2732, doi:10.1021/es9912933, 2000.

Rosenberg, P. D., Dean, A. R., Williams, P. I., Dorsey, J. R., Minikin, A., Pickering, M. A., and Petzold, A.: Particle sizing calibration with refractive index correction for light scattering optical particle counters and impacts upon PCASP and CDP data collected during the Fennec campaign, Atmos. Meas. Tech., 5, 1147–1163, doi:10.5194/amt-5-1147-2012, 2012.

Seiler, W. and Crutzen, P.: Estimates of gross and net fluxes of carbon between the biosphere and the atmosphere from biomass burning, Climatic Change, 2, 207–247, doi:10.1007/BF00137988, 1980.

Serreze, M. C., Holland, M. M., and Stroeve, J.: Perspectives on the Arctic's Shrinking Sea-Ice Cover, Science, 315, 1533–1536, doi:10.1126/science.1139426, 2007.

Shaw, G. E.: The Arctic Haze Phenomenon., B. Am. Meteorol. Soc., 76, 2403–2414, doi:10.1175/1520-0477(1995)076<2403:TAHP>2.0.CO;2, 1995.

Steinnes, E., Lukina, N., Nikonov, V., Aamlid, D., and Røyset, O.: A Gradient Study of 34 Elements in the Vicinity of a Copper-Nickel Smelter in the Kola Peninsula, Environ. Monit. Assess., 60, 71–88, doi:10.1023/A:1006165031985, 2000.

Ström, J., Umegård, J., Tørseth, K., Tunved, P., Hansson, H.-C., Holmén, K., Wismann, V., Herber, A., and König-Langlo, G.: One year of particle size distribution and aerosol chemical composition measurements at the Zeppelin Station, Svalbard, March 2000–March 2001, Phys. Chem. Earth, 28, 1181–1190, doi:10.1016/j.pce.2003.08.058, 2003.

Trembath, J. A.: Airborne CCN Measurements, PhD thesis, University of Manchester, Manchester, 2013.

Tunved, P., Ström, J., Krejci, R.: Arctic aerosol life cycle: linking aerosol size distributions observed between 2000 and 2010 with air mass transport and precipitation at Zeppelin station, Ny-Ålesund, Svalbard, Atmospheric Chemistry & Physics, 13, 3643–3660, doi:10.5194/acp-13-3643-2013, 2013.

Umo, N. S., Murray, B. J., Baeza-Romero, M. T., Jones, J. M., Lea-Langton, A. R., Malkin, T. L., O'Sullivan, D., Neve, L., Plane, J. M. C., and Williams, A.: Ice nucleation by combustion ash particles at conditions relevant to mixed-phase clouds, Atmos. Chem. Phys., 15, 5195–5210, doi:10.5194/acp-15-5195-2015, 2015.

Verlinde, J. Y., Harrington, J. Y., McFarquhar, G. M., Yannuzzi, V. T., Avramov, A., Greenberg, S., Johnson, N., Zhang, G., Poellot, M. R., Mather, J. H., Turner, D. D., Eloranta, E. W., Zak, B. D., Prenni, A. J., Daniel, J. S., Kok, G. L., Tobin, D. C., Holz, R., Sassen, K., Spangenberg, D., Minnis, P., Tooman, T. P., Ivey, M. D., Richardson, S. J., Bahrmann, C. P., Shupe, M., Demott, P. J., Heymsfield, A. J., and Schofield, R.: The Mixed-Phase Arctic Cloud Experiment, B. Am. Meteorol. Soc., 88, 205–221, doi:10.1175/BAMS-88-2-205, 2007.

Vihma, T., Pirazzini, R., Fer, I., Renfrew, I. A., Sedlar, J., Tjernström, M., Lüpkes, C., Nygård, T., Notz, D., Weiss, J., Marsan, D., Cheng, B., Birnbaum, G., Gerland, S., Chechin, D., and Gascard, J. C.: Advances in understanding and parameterization of small-scale physical processes in the marine Arctic climate system: a review, Atmos. Chem. Phys., 14, 9403–9450, doi:10.5194/acp-14-9403-2014, 2014.

Weinbruch, S., Wiesemann, D., Ebert, M., Schütze, K., Kallenborn, R., and Ström, J.: Chemical composition and sources of aerosol particles at Zeppelin Mountain (Ny Ålesund, Svalbard): An electron microscopy study, Atmos. Environ., 49, 142–150, doi:10.1016/j.atmosenv.2011.12.008, 2012.

Yakobi-Hancock, J. D., Ladino, L. A., and Abbatt, J. P. D.: Feldspar minerals as efficient deposition ice nuclei, Atmos. Chem. Phys., 13, 11175–11185, doi:10.5194/acp-13-11175-2013, 2013.

Yamaguchi, N., Ichijo, T., Sakotani, A., Baba, T., and Nasu, M.: Global Dispersion of Bacterial Cells on Asian Dust, Scientific Reports, 2, 525, doi:10.1038/srep00525, 2012.

Zhang, X. Y., Arimoto, R., Cao, J. J., An, Z. S., and Wang, D.: Atmospheric dust aerosol over the Tibetan Plateau, J. Geophys. Res., 106, 18471, doi:10.1029/2000JD900672, 2001.

Zhao, C., Klein, S. A., Xie, S., Liu, X., Boyle, J. S., and Zhang, Y.: Aerosol first indirect effects on non-precipitating low-level liquid cloud properties as simulated by CAM5 at ARM sites, Geophys. Res. Lett., 39, L08806, doi:10.1029/2012GL051213, 2012.

Zimmermann, F., Weinbruch, S., Schütz, L., Hofmann, H., Ebert, M., Kandler, K., and Worringen, A.: Ice nucleation properties of the most abundant mineral dust phases, J. Geophys. Res., 113, D23204, doi:10.1029/2008JD010655, 2008.

Table S1: Classification scheme adopted in this study. Similarly to Kandler et al. (2011), "All" stands for the sum of Na+Mg+Al+Si+P+S+Cl+K+Ca+Ti+Cr+Fe+Ni+Cu+Zn and square brackets indicate an interval of values. "All elements" represents each weight percentage unweighted. Kr2005: Krejci et al. (2005), K2007: Kandler et al. (2007), B2008: Behrenfeldt et al. (2008), G2010: Geng et al. (2010), H2010: Hand et al. (2010), K2011: Kandler et al. (2011). Source in bold: Direct copy of their criteria. Source in italics: Based upon their criteria.

Particle Class	Classification Criteria	Source
Carbonaceous	All elements/All<0.2, C+O>0.92 **OR** C+O>0.9, All elements/All<0.2 **AND** Mg/All≥0.1 **OR** Na/All≥0.1 **OR** S/All≥0.1	*G2010*
	Criteria for secondary Na-rich and Ammonium Sulphate	**K2011**
Biogenic	Criteria for biogenic	**K2011**
	C+O>0.9, Si/Cl<0.2, Na/Cl<0.3, Na/S<0.3 **AND** K/All≥0.2 **OR** P/All≥0.2 **OR** Cl/All≥0.2 **OR** (Ca+K)/All≥0.3 **OR** (Na+P+K)/All ≥ **OR** (Na+Mg+Zn)/All≥0.3	*Kr2005, G2010*
Sulphates	Criteria for NaS sulphates	**K2011**
Gypsum	(Ca+S)/All>0.5, Ca/S=[0.25;4], Si/Ca<0.5	**K2007**
	Criteria for Ca sulphates	**K2011**
Sulphates	S/All>0.4, Si/S<0.5, S>All elements	*K2007, H2010*
	Criteria for CaNaS	**K2011**
Ca-Rich	Ca/All>0.5, Si/Ca<0.5, Al/Ca<0.5, Ca>All elements	*H2010*
	Criteria for Ca- and CaMg-carbonates	**K2011**
	(Ca+Mg)/All>0.5, Mg/Ca=[0.33;3], Si/Ca<0.5, S/Ca<0.25, P/Ca<0.15	**K2007**
Phosphates	Criteria for phosphates	**K2011**
Fresh Chlorides	(Na+Cl)/All>0.5, S/Na<0.375, S/Cl<0.5, Si/Cl<0.2, Fe/Cl<0.5	**K2007**
	OR Na/Cl=[0.5;1.5], S/Cl<0.5, Si/Cl<0.2, S/Na<0.375, Fe/Cl<0.5	*Kr2005, G2010*
	Criteria for NaCl, KCl and other chlorides	**K2011**
Aged Chlorides	(Na+Cl)>0.4, S/Cl<5, S/Na<5, Si/Cl<0.5	*Kr2005, B2008*
	OR Cl/All=[0.1;1.1], Si/All<0.0699, Al/All<0.0099, Na/Cl<2, Mg/Cl<2, P/Cl<0.2, K/Cl<2, Ca/Cl<2, Ti/Cl<0.1, Cr/Cl<0.1, Fe/Cl<0.1	*K2011*
	Criteria for mixClS	**K2011**
Sulphates	Cl/S<0.5, Si/S<0.5, Ti/S<0.2, Cr/S<0.2, Fe/S<0.5, Ni/S<0.2, Cu/S<0.2, Zn/S<0.2	*K2007*
	Criteria for other sulphates	**K2011**
Metallic	Criteria for Fe, Ti, Fe-Ti and Al oxides	**K2011**
	OR Fe/All>0.3, Si/Fe<0.2, Al/Fe<0.2, Cl/Fe<0.2, Ti/Fe<1.33, Mg/Fe<0.2	**K2007**, *H2010*
	OR Ti/All>0.3, Na/Ti<1, Mg/Ti<1, Al/Ti<0.2, Si/Ti<0.2, S/Ti<1, Fe/Ti<1	**K2007**, *H2010*
Silicates	Criteria for quartz, SiAl, SiAlK, SiAlNa, SiAlNaCa, SiAlNaK, SiAlCaFeMg, SiAlKFeMg, SiAlFeMg, SiMgFe, SiMg, SiCaTi	**K2011**
	OR Si/All>0.2, Na/Si<0.7, Mg/Si<1.33, Al/Si<1.33, K/Si<0.5, Ca/Si<0.5, Ti/Si<0.5, Fe/Si<0.5, (P+S+Cl)/All<0.2	**K2007**
	OR Si/All≥0.6, S/Si<0.2, Cl/Si<0.2	*H2010*
	OR Si/All≥0.2, S/Si<0.2, Cl/Si<0.2 **AND** (Al+Si)/All≥0.6 **OR** (Si+Fe)/All≥0.6 **OR** (Al+Si+Fe)/All≥0.5 **OR** (Al+Si+Na)/All≥0.5 **OR** (Al+Si+Mg)/All≥0.5 **OR** (Al+Si+K)/All≥0.5 **OR** (Al+Si+Ca)/All≥0.5 **OR** (Al+Si+Ti)/All≥0.5	
	OR Si/All≥0.5, S/Si<0.2, Cl/Si<0.2 **AND** Mg/All≥0.1 **OR** K/All≥0.1 **OR** Ca/All≥0.1	
	OR (Si+Al)/All≥0.5, S/Si<0.2, Cl/Si<0.2 **AND** Mg/All≥0.1 **OR** K/All≥0.1 **OR** Ca/All≥0.1	
	OR (Si+Fe)/All≥0.5, S/Si<0.2, Cl/Si<0.2 **AND** Mg/All≥0.1 **OR** K/All≥0.1 **OR** Ca/All≥0.1	
	OR (Si+Al+Fe)/All≥0.5, S/Si<0.2, Cl/Si<0.2 **AND** Mg/All≥0.1 **OR** K/All≥0.1 **OR** Ca/All≥0.1	
Mixed Silicates	(Na+S+Mg+Al+Si+K+Ca)/All>0.7, S/Si=[0.6;2] **OR** (Al+Si)/All≥0.6, S/Si>0.2	**K2007**, *H2010*
	OR Si/All≥0.2, Na/Si<0.7, Mg/Si<1.33, Al/Si<1.33, K/Si<0.5, Ca/Si<0.5, Ti/Si<0.5, Fe/Si<0.5, (P+Cl)/All<0.2, S/All>0.2	*K2007*
	OR Si/All≥0.1, S/Si>0.2 **AND** (S+Si)/All≥0.5 **OR** (S+Si+Al)/All≥0.5 **OR** (Si+S+Fe)/All≥0.5 **OR** (Si+S+Al+Fe)/All≥0.5	
	OR Si/All≥0.1, (Si+S)/All≥0.4, S/Si>0.2 **AND** Mg/All≥0.1 **OR** K/All≥0.1 **OR** Ca/All≥0.1	
	OR Si/All≥0.1, (Si+S+Al)/All≥0.4, S/Si>0.2 **AND** Mg/All≥0.1 **OR** K/All≥0.1 **OR** Ca/All≥0.1	
	OR Si/All≥0.1, (Si+S+Fe)/All≥0.4, S/Si>0.2 **AND** Mg/All≥0.1 **OR** K/All≥0.1 **OR** Ca/All≥0.1	
	OR Si/All≥0.1, (Si+S+Fe+Al)/All≥0.4, S/Si>0.2 **AND** Mg/All≥0.1 **OR** K/All≥0.1 **OR** Ca/All≥0.1	
	OR Fe/All>0.15, Si/Fe<1, Ti/Fe<1.33, (Fe+S)/All>0.4 **OR** Ti/All>0.3, Na/Ti<1, Mg/Ti<1, Al/Ti<1, Si/Ti<1, Fe/Si<1, (Ti+S)/All>0.4 **OR** (Ti+S)/All>0.5	*K2007*
	Criteria for mixSiS, mixAlSiS, mixNaClSi, mixNaClSiAl, mixCaSi, mixCaAlSi	**K2011**
Fresh Chlorides	(Na+Cl+Ca)/All≥0.5, Na/Cl=[0.2;1.1], Si/Cl<0.2, S/Cl<0.2	
Aged Chlorides	(Na+Cl+Ca+S)/All≥0.5, Na/Cl=[0.1;1.1], Si/Cl<0.2, S/Cl>0.2	
	OR Cl/All=[0.1;1.1], Si/Cl<0.1, S/Cl>0.2, Cr/Cl<1	
Metallic	(Fe+Ni+Cr+Cu+Zn)/All>0.5, Si/(Fe+Ni+Cu+Zn)<0.05 **OR** Zn/All=[0.2;1.1] **OR** Cu/All=[0.2;1.1] **OR** Cr/All=[0.2;1.1] **OR** Ni/All=[0.2;1.1] **OR** Cu>All elements	
Silicates	Mg/All=[0.35;1.1], Si≥0.1	*K2011*
Phosphates	P/All=[0.1;1.1], P>All elements	
Silicates	Si/All=[0.1;1.1]	**K2011**
Metallic	Al/All=[0.1;1.1]	
Silicates	(Al+Si)/All=[0.2;1.1], Si≥0.1	
Fresh Chlorides	Cl/All=[0.1;1.1]	
Biomass Tracers	K/All=[0.25;1.1]	**K2011**
Ca-Rich	Ca/All=[0.2;1.1]	*K2011*
Other	Particles not classified by these criteria	

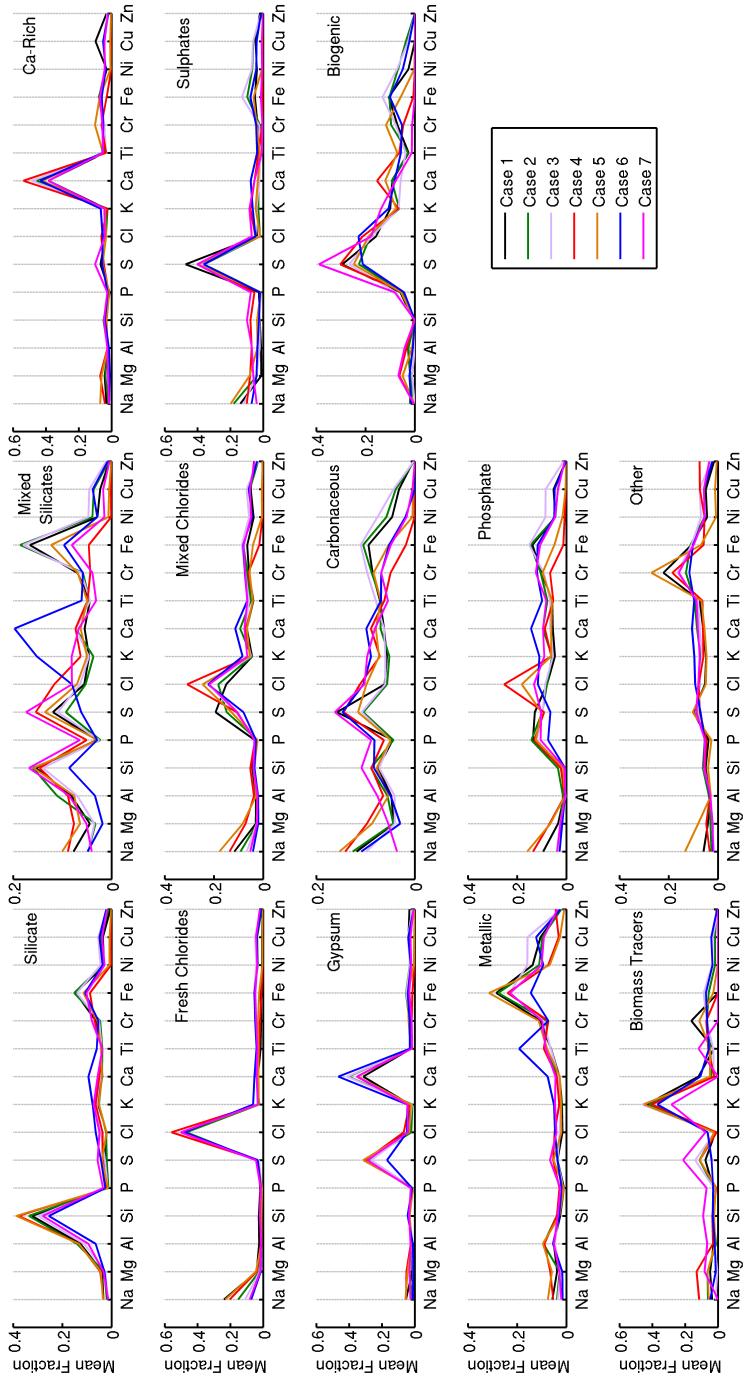

Figure S2: Mean elemental fractions of each particle category, normalised by the summed contributions from all elements except C and O. Variability is seen most clearly in the mixed categories, with consistency amongst the well-defined categories (e.g. Ca-rich)